Land Use Policy xxx (xxxx) xxx

Contents lists available at ScienceDirect

Land Use Policy

journal homepage: www.elsevier.com/locate/landusepol

Post-fire practices benefits on vegetation recovery and soil conservation in a Mediterranean area

Manuel López-Vicente [a,b,*], Artemi Cerdà [c], Henk Kramer [d], Saskia Keesstra [a]

[a] Team Soil, Water and Land Use, Wageningen Environmental Research, Droevendaalsesteeg 3, Wageningen 6708RC, The Netherlands
[b] AQUATERRA Research Group, Advanced Scientific Research Centre, University of A Coruña, CICA-UDC, As Carballeiras s/n, Campus de Elviña, La Coruña 15071, Spain
[c] Soil Erosion and Degradation Research Group, Department of Geography, Valencia University, Blasco Ibàñez 28, Valencia 46010, Spain
[d] Team Earth Informatics, Wageningen Environmental Research, Droevendaalsesteeg 3, Wageningen 6708RC, The Netherlands

ARTICLE INFO

Keywords:
Forest fire
Log erosion barrier
Vegetation recovery
Sediment connectivity
Drone imagery

ABSTRACT

Post-fire practices (PFP) aim to reduce soil erosion and favour vegetation recovery, but their effectiveness is spatially heterogeneous and under debate because of the economic and environmental costs. This study evaluates the different changes (Δ) of canopy cover (CC), sediment connectivity (SC) and local topography in four areas affected by the Pinet fire in eastern Spain (August 8th, 2018) and managed with: totally burnt with tree removal and long log erosion barriers (LEBs) (Pinet-1), partially burnt without PFP (Pinet-2), totally burnt with tree removal and short LEBs (Pinet-3), and totally burnt without PFP (Pinet-4). An unburnt nearby area was used as control site (Pinet-5). High-resolution images obtained before the fire and during two drone flights after the fire (10.5 and 5.5 months after the fire and PFP; and 18 and 13 months after the fire and PFP) were analysed; and LiDAR- and SfM-derived digital elevation models used to compute the Aggregated Index of SC (AICv2). After correcting calculations, because of the different input sources, and excluding the forest roads ($\overline{x}$=3.6% of the total surface), CC in the first post-fire scenario was of 25.5% (−40.4% with respect to the pre-fire scenario), 14.5% (−68.4%), 23.8% (−43.7%), 26.9% (−26.5%) and 29.6% (−32.7%) in Pinet-1, P-2_totally_burnt, P-2_partially_burnt, P-3 and P-4; and ΔCC among the drone flights were of +2.45%, +0.02% and +10.54% in Pinet-1, Pinet-3 and Pinet-4. The annual CC recovery rate decrease from 27.5% to 19.1% per year between the first and the second post-fire scenario, indicating a quick vegetation recovery, especially in the first year, and considering the surface area covered by rocks ($\overline{x}$=16.3%). Topographic changes indicated that not install LEBs favoured shorter flow length pathways after the fire, and thus, runoff will flow faster to cover the same area, achieving higher velocity and thus soil detachment capacity. Sediment connectivity increased in all burnt sub-sites after the fire ($\overline{\Delta 1}$=+32.4%), but the increments in the two sub-sites with LEBs were 36% lower than the increase in the sub-sites without LEBs. The increase of connectivity in the first and second post-fire scenarios was −32% and −45% in the sub-site with long LEBs compared with the sub-site with short LEBs. Overall, LEBs effectively favoured vegetation recovery, lengthened overland flow pathways, and reduced sediment transport in the early months, but their usefulness was not as pronounced during the second post-fire year, although these results may be influenced by the Mediterranean conditions of the site.

1. Introduction

Forest fires devour vegetation and modify ground conditions, causing significant changes on soil properties, such as soil water infiltration and hydrophobicity (Jiménez-Morillo et al., 2017), time to ponding (Ebel and Moody, 2017) and runoff generation (Fernández et al., 2019a), soil erosion and transport (Sheridan et al., 2011), contaminant –mainly ash– delivery (García-Comendador et al., 2017) and ecosystem services (Robinne et al., 2020). Despite wildfires are among the mechanisms that regulate the biosphere and constitute one of the major pathways to release nutrients again available to plants (Pausas and Bond, 2020), their socio-economic consequences at short- and medium-term are not desirable (Stephenson et al., 2013). Forest fires cause casualties and large economic damages (Bonazountas et al., 2007;

* Corresponding author at: Team Soil, Water and Land Use, Wageningen Environmental Research, Droevendaalsesteeg 3, Wageningen 6708RC, The Netherlands.
E-mail address: manuel.lopez.vicente@udc.es (M. López-Vicente).

https://doi.org/10.1016/j.landusepol.2021.105776
Received 13 July 2021; Received in revised form 15 September 2021; Accepted 20 September 2021

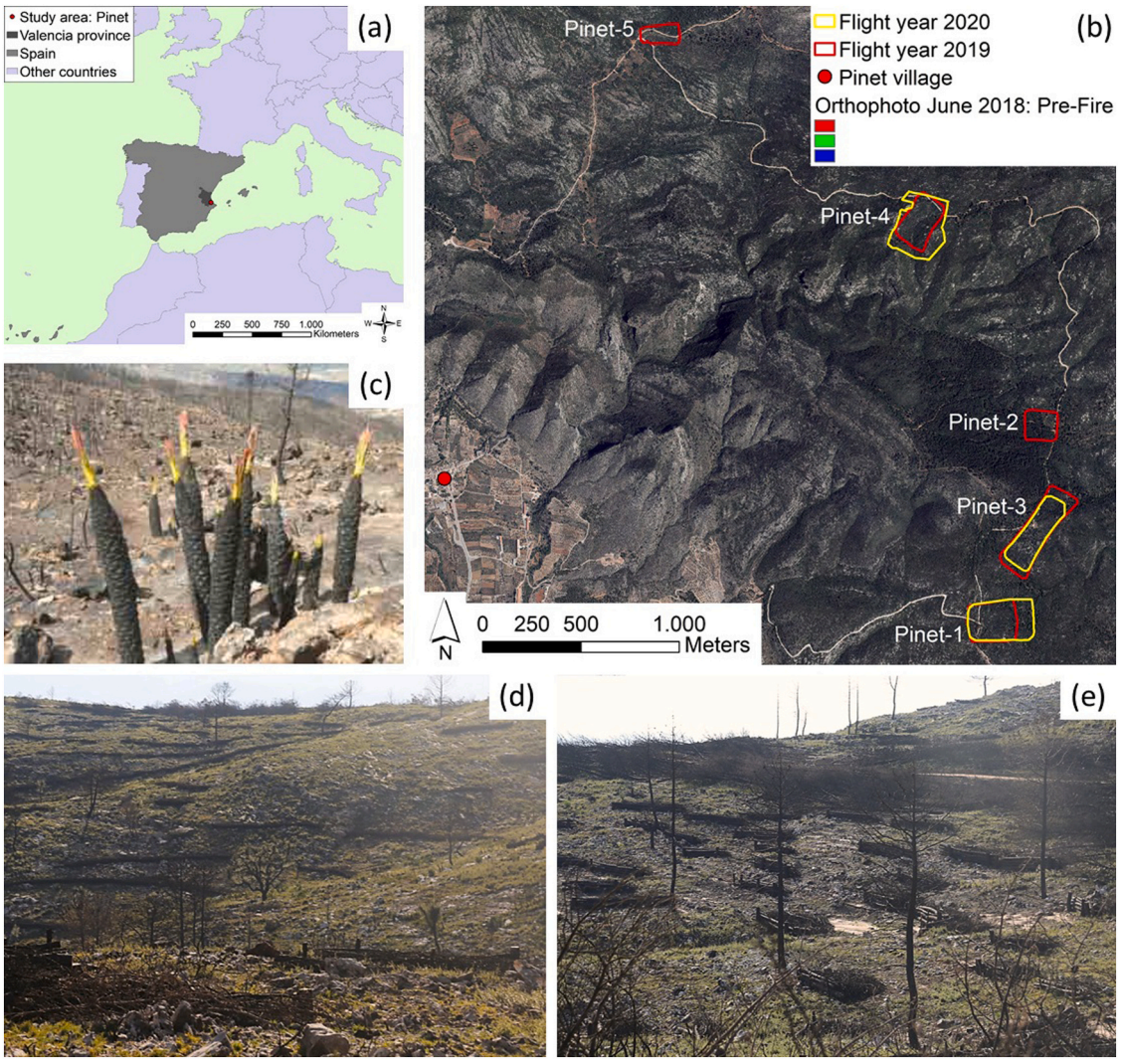

Fig. 1. Location of the study are in eastern Spain (a). Aerial image of the study area showing the boundaries of the five sites and drone flights done in June 2019 and February 2020 (b). Dwarf palm (*Chamaerops humilis*) regrown (c). Photographs of the Pinet-1 (d) and Pinet-3 (e) sites showing the long and short log-barriers, respectively.

Diakakis et al., 2016). Besides, wildfires creates greenhouse gas (GHG) emissions, affecting the ecosystem carbon balance (Volkova et al., 2021).

Regarding soil erosion and vegetation recovery, post-fire response includes different alternatives: Salvage logging (burnt-tree removal), installation of soil erosion barriers with natural or man-made materials at hillslope (e.g. log erosion barriers, contour-felled logs) and catchment (e.g. check-dams) scales, seeding, hydroseeding, tree plantation, mulching (agricultural straw, wood strands, wood shreds, etc.) or allow nature to recover, which is named here as natural regeneration (Beghin et al., 2010; Robichaud et al., 2010; Albert-Belda et al., 2019). Among the factors influencing vegetation recovery, fire intensity and occurrence of repeated fires are two of the most important, extending the time needed to reach pre-disturbance values in the worst-case scenarios (Ruokolainen and Salo, 2009; Keesstra et al., 2017). Fire effects on vegetation also depend on plant species, appearing different responses –in terms of post-fire resprouting, growth and productivity– in the same area in the patches with native or invasive species (Laushman et al., 2020).

The effectiveness of post-fire practices (PFP) is not homogeneous in terms of spatial variability (Lopez Ortiz et al., 2019), efficiency (de Figueiredo et al., 2017) and lifespan (Robichaud et al., 2019), owing to physiographic conditions (north- and south-facing slopes, slope gradient thresholds, areas with shallow soils), occurrence of low-, medium- and high-intensity rainfall events, and the presence of gaps between logs or branches that allow runoff to flow through. The use of log erosion barriers (LEBs) is certainly widespread in fire-affected areas under distinct plant communities and land uses, such as in sub-urban areas –where houses and linear infrastructures are mixed with forest– (Wittenberg et al., 2020), semi-arid Mediterranean landscapes with stony soils (Badía et al., 2015), and mixed pine/oak headwater catchments in California (Wohlgemuth et al., 2001). However, in other areas LEBs did not reduce significantly post-fire soil erosion, and rates varied in the same range as that observed in areas with no intervention (Fernández et al., 2019b). Therefore, there is debate about the effectiveness of LEBs and further research is needed to assess the appropriateness of their installation or not.

Despite implementation of multiple PFP, in Mediterranean areas, natural regeneration of pine forest exhibits an intermittent temporal pattern, associated with climate-mediated bottlenecks, seed predation and initial seedling survival, which should be aggravated under drier scenarios (Calama et al., 2017). Furthermore, repeated forest fires have seriously damaged both original and recovered vegetation in the last few decades in many Mediterranean areas, such as in pine plantations in Portugal (Nunes et al., 2016; Van Eck et al., 2016), in fire-adapted conifers (e.g. *Pinus halepensis* Mill. – Aleppo pine) in Spain (Budde et al.,

Table 1
Main characteristics of the fire, post-fire practices and drone flights in the five sub-sites.

Sub-site	Burnt area		Post-fire practices				Drone flight date	
	Date	Extension	Date	BTR	LEBs		Flight #1	Flight #2
Pinet-1	6–12/08/2018	Total	01/2019	Yes	Yes	Long	27/06/2019	03/02/2020
Pinet-2	6–12/08/2018	Partial	No	No	No	No	27/06/2019	No flight
Pinet-3	6–12/08/2018	Total	01/2019	Yes	Yes	Short	27/06/2019	03/02/2020
Pinet-4	6–12/08/2018	Total	No	No	No	No	27/06/2019	03/02/2020
Pinet-5	Unburnt	Unburnt	No	No	No	No	27/06/2019	No flight
Relative dates			5 months after the fire				10.5 months AF 5.5 months APFP	18 months AF 13 months APFP

BTR: Burnt tree removal; LEBs: Log erosion barriers; AF: After the fire; APFP: After post-fire management practices.

2017), in Italian urbanised landscapes (Elia et al., 2020), in drylands in Greece and Cyprus with shallow soils and a long history of anthropogenic pressure (Jucker Riva et al., 2017), and in mixed-conifer landscapes in California where black oaks are resilient to recurring wildfire while conifer regeneration suffered complete mortality (Nemens et al., 2018). The accumulated effect of these episodes on vegetation together with the current trend of more severe and frequent droughts in Mediterranean countries is determining the plant response of ecosystems (Francos et al., 2016; Vega et al., 2018). Thus, the evaluation at high spatial resolution of the vegetation recovery rates in areas affected by multiple fires is a research need (Cerdà et al., 2017; Machida et al., 2021).

In fire-affected areas, the use of remote sensing imagery to characterise vegetation structure, composition and ratios (e.g. Leaf Area Index [LAI], Normalized Difference Vegetation Index [NDVI]) and to assess burnt severity classes (e.g. delta normalized burn ratio [dNBR], normalized multi-band drought index [NMDI]) has become a common tool (Martínez-Murillo and López-Vicente, 2018; Viedma et al., 2020). In the last decade, the use of unmanned aerial vehicles (UAV) –also known as drones– has been increasing and become popular, allowing the evaluation of vegetation patterns, monitoring of fires and characterization of post-fire scenarios at very high spatial resolution (at centimetre scale). For instance, in the study of fire severity in a red pine forest in South Korea (Shin et al., 2019), in the identification of the edges of unburnt areas (Talucci et al., 2020), for the accurate assessment of soil erosion features developed after fires by using Structure-from-Motion photogrammetry (Ellett et al., 2019), and for quantifying the effectiveness of erosion barriers to minimize sediment connectivity (López-Vicente et al., 2021). The term 'sediment connectivity' (SC) has become a key issue in the study of processes acting in hydro-geomorphic systems and a useful concept to evaluate the efficiency of water and sediment transfer through a catchment or hydrological unit (Cavalli et al., 2019).

This study aims to evaluate the impact of post-fire management practices (PFP) on (i) the vegetation recovery rates; and (ii) the magnitude of sediment connectivity in four sub-sites affected by the same wildfire but in a different way (partially or completely burnt), and including different PFP (no practice, short and long LEBs). We hypothesized that doing nothing after the fire could be as effective as installing LEBs in terms of vegetation recovery and sediment connectivity. The results of this study will be of interest to better plan future management strategies in Mediterranean forest affected by wildfires.

2. Materials and methods

2.1. Fire characteristics, study area and post-fire practices

The forest fire, caused by lightning and called "Wildfire of 'Llutxent 2018'", started on August 6, 2018 and lasted six days; it was extinguished on August 12. It affected seven municipalities within the La Vall d'Albaida and La Safor district in the Valencia province (Ador, Barx, Gandia, Llutxent, Pinet, Quatretonda and Rótova) and burnt a total area of 3270 ha (3146 ha of forest land) (Alloza et al., 2018) in the province of Valencia, eastern Spain (Fig. 1a). High temperatures in the days before the fire, wind gusts that reached 50 km per hour, and dry soil and vegetation conditions favoured the rapid expansion of the fire. In the corresponding hydrological year (since 1st October 2017), the total accumulated rainfall depth was 281.3 mm against the average record in the area that reaches 539.7 mm. Besides, topography is hilly, with a mean slope gradient of 22%, which hindered access of machinery. The fire-affected area is located within the 'El Surar' natural place, near the village of Pinet (Fig. 1b), and in the heart of the fire affected land. Most of the burnt area was affected in previous fires over the last 40 years, and thus, the affected vegetation did not have a great stand, although vegetation density was high in some areas.

Burnt vegetation mainly consisted of scrubland (90%), dominated by kermes oak (*Quercus coccifera*) with presence of rosemary (*Rosmarinus officinalis*), dwarf palm (*Chamaerops humilis*), mastic tree (*Pistacia lentiscus*), heather (*Erica multiflora*) and isolated individuals of *Erica scoparia* –a typical heather species of decarbonated soils– (Fig. 1c). Wooded areas were covered by Aleppo pine (*Pinus halepensis*) and small patches of maritime pine (*Pinus pinaster*), holm oak (*Quercus ilex*), and cork oak (*Quercus suber*). The rock outcrops are mainly limestones and dolomites. The soil in the study area is classified as Cambisol, with minor areas as Leptosol, with a significant content of coarse fragments, ca. 19.5% per volume (source: https://soilgrids.org/). Soil bulk density ranges between 1.15 (topsoil) and 1.44 (at 50-cm depth) g cm^{-3}; and soil texture is loam. The organic carbon density ranges between 4.2% (topsoil) and 1.4% (at 50-cm depth). We did not observe significant changes in the soil type along the study area.

PFP were performed from November 2018 until March 2019 over the entire area. In the selected sub-sites of this study, the restoration works were done in January 2019, and PFP included removal of burnt trees and installation of LEBs that were made of branches (Fig. 1d,e).

2.2. Drone flights, sub-sites and temporal scenarios

In this study, we focussed on five sub-sites (Table 1). Each one represents a different combination of fire-affected area and PFP, namely: Pinet-1, totally burnt with tree removal and installation of 74 long LEBs that have a mean length of 20.5 m ($\tilde{x}$=15.9 m; σ = 15.7 m) (16.5 LEBs / ha; 339.5 m / ha); the cut trunks and chopped branches occupy a mean area of 30.1 m^2 / LEB (.=21.0 m^2 / LEB; σ = 26.8 m^2 / LEB) (484.7 m^2 / ha). Pinet-2, without PFP and with different grades of fire severity, namely: partially burnt (52.7% of the total sub-site area) and totally burnt (41.7%); the remaining 5.5% corresponds to the unpaved forest road. Pinet-3, totally burnt with tree removal and installation of 105 short LEBs (.=5.8 m; $\tilde{x}$=5.0 m; σ = 3.1 m) (21.2 LEBs / ha; 122.1 m / ha); the burnt vegetation remnants occupy a mean area of 10.8 m^2 / LEB ($\tilde{x}$=8.8 m^2 / LEB; σ = 9.5 m^2 / LEB) (233.4 m^2 / ha). Pinet-4, totally burnt without PFP. An unburnt nearby area, called Pinet-5, was used as control site. The slope gradient is comparable among the sub-sites, with mean values of 25.3% (σ = 19.8%), 21.8% (σ = 19.0%), 26.1% (σ = 19.0%), 59.1% (σ = 30.9%) and 32.9% (σ = 22.5%) in Pinet-1,

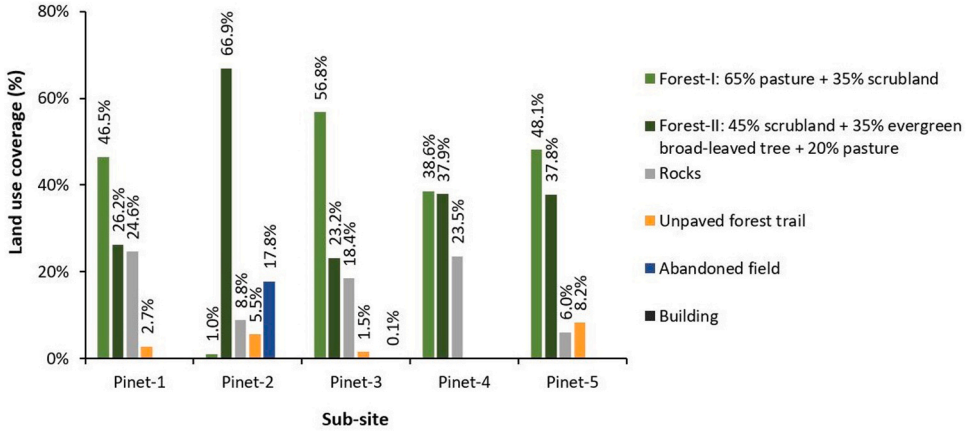

Fig. 2. Occupied area by each land use and land cover before the forest fire.

Pinet-2, Pinet-3, Pinet-4 and Pinet-5, respectively. After the PFP, two drone flights were done, namely: on June 27, 2019 (scenario Flight-1; 10.5 and 5.5 months after the fire and PFP, respectively) and February 3, 2020 (scenario Flight-2; 18 and 13 months after the fire and PFP, respectively). Therefore, the time lapse between the two flights was of 7.5 months. We used a 'DJI – Phantom 4′ drone (technical specifications can be found in the website of the manufacturer).

A pre-fire scenario is necessary in order to assess different changes in vegetation recovery, sediment connectivity and local topographic parameters. A orthophoto (taken in June 2018 at 0.25 m of spatial resolution), and the LiDAR-based digital elevation model (DEM; at 2 × 2 m of grid cell size) generated by the Spanish National Centre of Geographic Information (IGN) are the sources to characterize the pre-fire scenario. The aerial orthophoto was taken less than two months before the fire, and thus, the derived information about vegetation can be considered as representative of the existing conditions when the forest fire started. The land use and land cover map is generated by using the SIOSE land cover map provided by IGN. The structure of each SIOSE polygon came as the result of the combination of the different covertures inside that polygon (conifer forest, palms, shrubs…) with different percentages linked to each land use (e.g. 60% of conifer forest; 25% of dense shrubs; and 15% of herbs). In spite of the detailed map, some improvements were made such as the addition of the forest trails, abandoned fields, buildings and rocks (see Appendix A). These features occupy a significant percentage of the total area, and thus, they are relevant in terms of soil erosion and preferential flow pathways in the landscape (Salesa et al., 2019) (Fig. 2).

2.3. Image processing and vegetation recovery assessment

A total of 1510 pictures were taken in the first survey (Flight-1), and cover an area of 199,426 m^2 including the five sub-site. Another set of 2141 pictures were obtained in the second survey (Flight-2) that cover an area of 185,494 m^2 including three sub-sites (Pinet-1, −3 and −4). The generated orthomosaics –one per sub-site and date– had a spatial resolution (width of the pixel) that ranged between 0.008 and 0.040 m. Before generating the Structure-from-Motion (SfM) photogrammetry-derived DEM, point clouds representing vegetation (e.g., trunks and branches) were removed. In this study, we used the following five-step process to obtain accurate and comparable DEMs: (I) photos processing and generation of the point cloud with *Pix4Dmapper* (Pix4D S.A. Prilly, Switzerland); (II) ground point classification with *LAStools* (rapidlasso GmbH. Gilching, Germany); (III) manual correction of ground point classification with *ArcGIS Pro* (Esri. Redlands, USA) in order to remove any pixel that was wrongly classified as ground in step II; (IV) DEM generation, at a spatial resolution (width of the pixel) that ranged between 0.011 and 0.061 m, by interpolating the ground points; and (V) resample the SfM-DEMs at the same pixel size, at 0.1 × 0.1 m, by using the nearest method, which is a fast interpolation method that do not change the values of the cells and the maximum spatial error is one-half the cell size. We chose this spatial resolution, in order to ensure overland flow continuity and to avoid errors associated with artificial artefacts (see Appendix A). Finally, the small local depressions were removed using the "Fill Sinks XXL (Wang & Liu)" module (available in *SAGA*) without adding unrepresentative flat surfaces. A minimum gradient of 0.01° was set to ensure flow routing across the filled sinks.

In order to obtain comparable areas at each sub-site over time, and taking into account the minor differences in the boundaries of each flight survey (see Appendix A), we intersected the boundaries of the two flights, obtaining the working-area of each sub-site (Fig. 3). All parameters and estimations of vegetation recovery, sediment connectivity and topographic metrics were performed within the working-area, excluding the remaining area. The extension of the working-area was of 44,737, 23,284, 49,459, 29,333 and 16,307 m^2 in Pinet-1, Pinet-2, Pinet-3, Pinet-4 and Pinet-5, respectively.

The high contrast levels between the colours of the burnt vegetation (dark grey and brown), rock outcrops (light grey and white), soil (brown and orange), LEBs (dark brown), and new vegetation (green) allowed us to estimate the soil surface area covered by the new vegetation –growth after the fire– using the obtained orthomosaics. The RGB images were converted to palette (PCT) images using the Tool 'conversion' of *QGIS* (a free and open source GIS). This tool classifies pixels into groups of similar colour. After analysing the converted images (excluding the pixels outside the intersected area) in the areas with (i) new vegetation, (ii) the shadows within the patches with new vegetation; (iii) rocks, and (iv) LEBs; with different ranges of colours (from 4 to 22), we found that 18 colours were the best choice (Fig. 4). Between 4 and 8 colours, the "green" pixels did not include all areas with new vegetation; between 9 and 16 colours, the "green" pixels included all areas with new vegetation and others without vegetation but having similar colours; and between 17 and 22 colours, the "green" pixels only appear within the patches with vegetation. In order to refine the selection of the best option, we extended the analysed to the areas with rocks: between 4 and 5 colours, the "white" pixels clearly overestimated the ground area covered with rocks; between 6 and 16 colours, the "white" pixels slightly overestimated the ground area covered with rocks; and between 17 and 22 colours, the "white" pixels matches well with the actual areas with rocks. Thus, similar results were obtained using vegetation- and rock-covered areas, and the final decision was made after looking in detail the images with 17–22 colours (more details in Supplementary File).

2.4. Sediment connectivity patterns and changes

In order to assess the impedance to sediment transport associated with the different post-fire practices and vegetation recovery at each

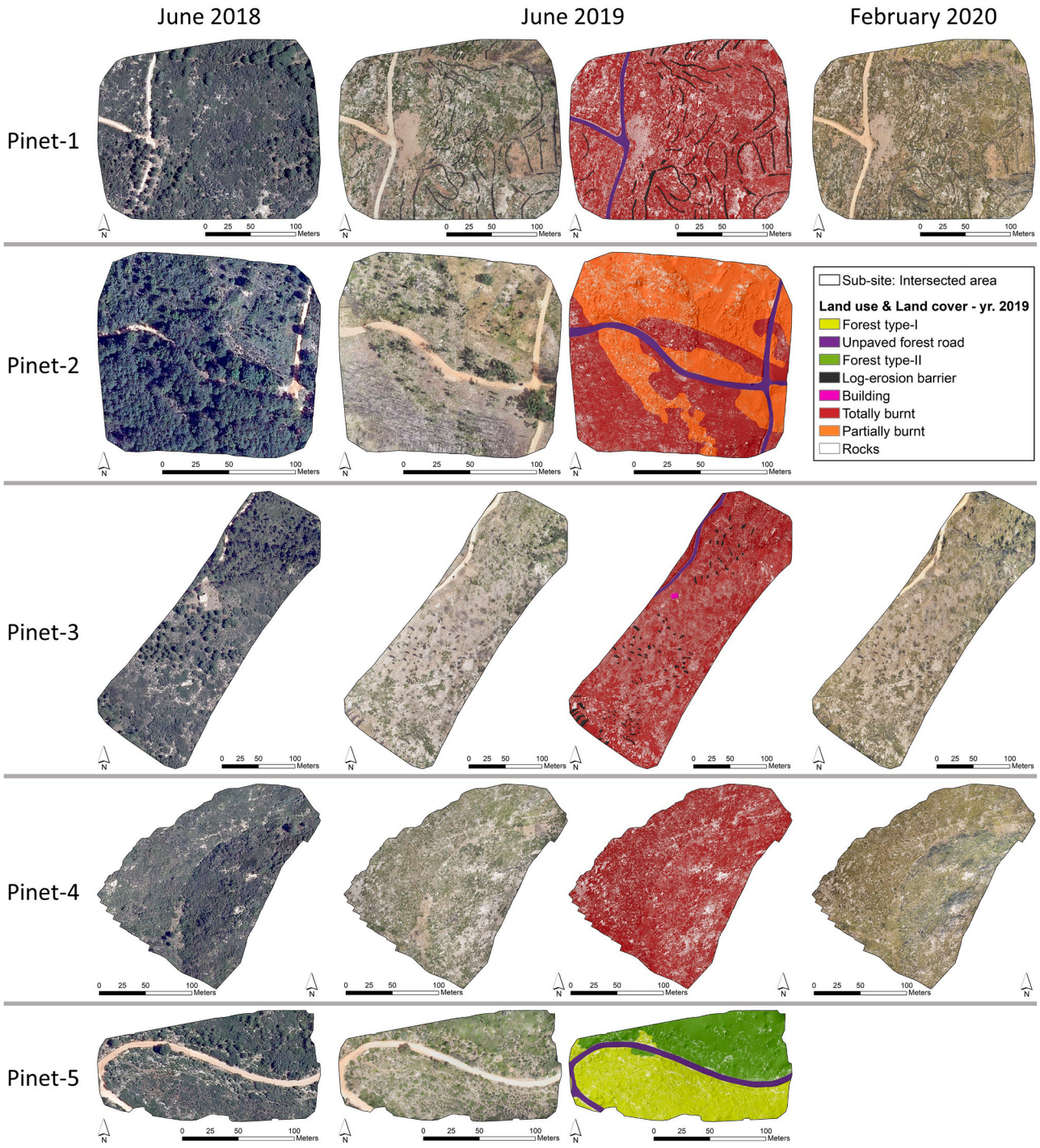

Fig. 3. Aerial orthophoto and orthomosaics of the intersected area in the five sub-sites and over the three temporal scenarios. The land-use map of each sub-site of the second scenario (June 2019) is also included. In the legend: Forest type-I: 65% pasture +35% scrubland; and Forest type-II: 45% scrubland +35% evergreen broad-leaved tree +20% pasture.

sub-site, we ran a simplified version of the aggregated index of sediment connectivity (AIC). This index was proposed by López-Vicente and Ben-Salem (2019) and recently enhanced by López-Vicente et al. (2021). This index accounts for the role played by the drainage area and flow path characteristics at each pixel. The downslope module ($\boldsymbol{D_{dn}}$) contemplates the probability that runoff and sediment arrive at a user-defined computation target (e.g. sink, check-dam, pond, outlet, channel, stream system). The upslope module ($\boldsymbol{D_{up}}$) represents the potential for downward routing of overland flow occurring upslope and also implements a "stream power"-like approach, taking into account the weighting factors and size of the drainage area:

$$AIC_k = \log_{10}\left(\frac{D_{up,k}}{D_{dn,k}}\right) = \log_{10}\left(\frac{\overline{AWC_t}\cdot\sqrt{A_k}}{\sum_{k=i}^{n}\frac{d_i}{AWC_i}}\right) \quad (1)$$

$$AWC_i = R_{ti}\cdot RT_i\cdot C_{ti}\cdot K_{Pi}\cdot S_i \quad (2)$$

where $\boldsymbol{AWC}$ is the aggregated weighting factor at catchment scale, $\boldsymbol{A}$ is the upslope drainage area (m^2), $\boldsymbol{d_i}$ is the length of the ith cell along the

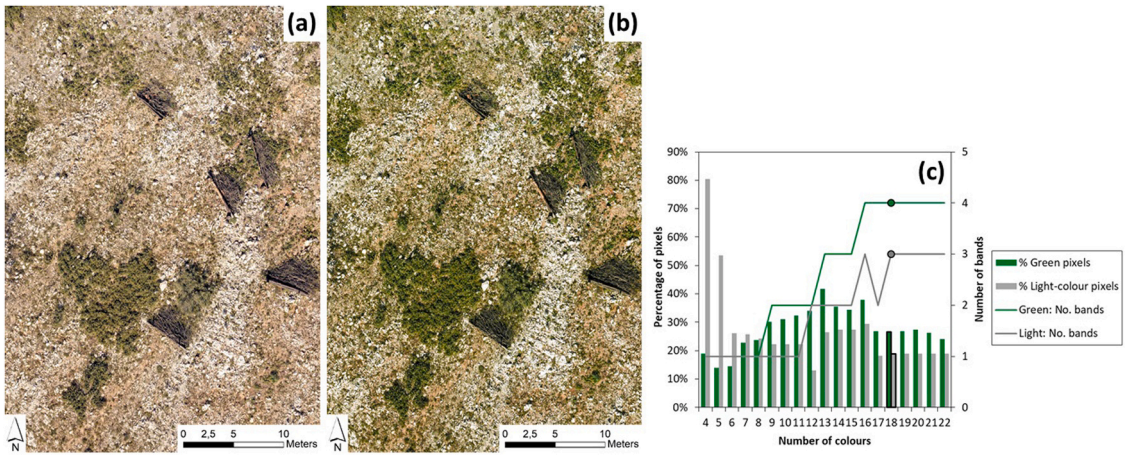

Fig. 4. Detail of the original RGB image of Pinet-3, taken with the drone in February 2020 (a), and 18-colour converted PCT image of the same area (b). Percentage of green (associated to the new vegetation) and light-colour (associated to rocks) pixels obtained in the different conversions (from 4 to 22 ranges of colours) of the intersected image of Pinet-3 taken in February 2020 (c).

Table 2
Estimated canopy cover (CC) and ground cover (GC) values at the 25 land covers identified in the five sub-sites and over the three temporal scenarios.

Pre-fire CODE[a]	Land use	Sub-site	CC / GC (%)		
			2018	2019	2020
3	(45%Scrubland+35%EvergreenBroadLeavedTree+20%PST)	P1	45.23%	ND	ND
3	(45%Scrubland+35%EvergreenBroadLeavedTree+20%PST)	P2	43.99%	ND	ND
3	(45%Scrubland+35%EvergreenBroadLeavedTree+20%PST)	P3	35.17%	ND	ND
3	(45%Scrubland+35%EvergreenBroadLeavedTree+20%PST)	P4	38.65%	ND	ND
3	(45%Scrubland+35%EvergreenBroadLeavedTree+20%PST)	P5	54.99%	59.63%	ND
1	(35%Scrubland+65%PST)	P1	41.47%	ND	ND
1	(35%Scrubland+65%PST)	P2	50.44%	ND	ND
1	(35%Scrubland+65%PST)	P3	37.07%	ND	ND
1	(35%Scrubland+65%PST)	P4	49.15%	ND	ND
1	(35%Scrubland+65%PST)	P5	52.52%	48.97%	ND
33	Abandoned field	P2	43.01%	ND	ND
2	Unpaved forest road	P1-P5	0%[b]	0%[b]	0%[b]
5	Building	P3	100%[b]	100%[b]	100%[b]
99	Rocks	P1-P5	0%[b]	0%[b]	0%[b]
4	Log-erosion barrier	P1, P3	ND	> 95%	> 95%
44	Totally burnt	P1	ND	25.53%	26.15%
44	Totally burnt	P2	ND	14.45%	ND
44	Totally burnt	P3	ND	26.87%	26.87%
44	Totally burnt	P4	ND	29.59%	32.71%
55	Partially burnt	P2	ND	23.82%	ND

ND: No data;
[a] These codes were assigned by the authors of this study during the pre-processing tasks of the AIC inputs, and they only have system setup meaning;
[b] These values were suggested taking into account the role played by the land cover regarding overland flow.

downslope path (m), $\boldsymbol{R_t}$ is the normalized rainfall erosivity factor for the period $\boldsymbol{t}$ (values between 0 and 1), $\boldsymbol{RT}$ is the roughness of the terrain factor (normalized values between 0 and 1), $\boldsymbol{C_t}$ is the vegetation (crop and natural vegetation) management factor for the period $\boldsymbol{t}$ (values between 0 and 1), $\boldsymbol{K_P}$ is the soil permeability factor (normalized values between 0 and 1) and $\boldsymbol{S}$ is the slope gradient (m / m). The subscript $\boldsymbol{K}$ indicates that each cell '$\boldsymbol{i}$' of the catchment has its own value of sediment connectivity. The AIC approach is defined in the range of $[-\infty, +\infty]$ and connectivity increases when the index tends to grow towards $+\infty$.

The weighting component $\boldsymbol{AWC}$ calculates the impedance to runoff and sediment fluxes due to properties of the local physiographic conditions. The $\boldsymbol{C}$-factor of the (R)USLE-family soil erosion models reflects the effect of the vegetation, land uses and tillage and management practices on the soil erosion rates (Nearing, 2013). In this study, we combined the information of the pre-fire vegetation (six land uses; see Table 2) with the estimated values of canopy cover at each sub-site and temporal scenarios, obtaining a total of 25 different land covers (Table 2). Then, the C-factors (see Appendix B) were designated to each land cover using the values proposed by Panagos et al. (2015) for the CORINE Land Cover datasets (CLC, 2016): Agro-forestry area (CLC class 244), sclerophyllous vegetation (CLC class 323), transitional woodland-shrub (CLC class 324), bare rocks (CLC class 332), and recent burnt areas (CLC class 334). For the unpaved forest road (C=0.5027) and the log erosion barriers (C=0.001; maximum flow impedance), we used the C-factors proposed by López-Vicente and Navas (2009) and González-Romero et al. (2021), respectively.

The $\boldsymbol{RT}$ factor estimates the role of the microtopography homogeneity/ heterogeneity on the impedance of overland flow. In order to minimize the temporal variability between the evaluated scenarios in this study and to focus the analysis on the sole effect of the soil erosion barriers and canopy cover recovery, the rainfall erosivity factor was set to a value of $\boldsymbol{R_t} = 1$ in the three scenarios. The $\boldsymbol{K_P}$ factor allows to account the spatially distributed influence of the soil physical properties on the hydrological response of the soil. In this study, the $\boldsymbol{K_P}$ factor was set to a constant value of $\boldsymbol{K_P} = 1$ in the three scenarios and five sub-sites due to two reasons: (I) to reduce the spatial variability of the AIC values,

Table 3
Percentage of the ground surface covered with vegetation (canopy cover: CC; in %) and temporal changes of CC (in %) observed in the two drone flights, obtained in the five sub-sites during the three temporal scenarios: Pre-fire (06/2018), Flight-1 (06/2019) and Flight-2 (02/2020).

Sub-site	Burnt degree	PFP	Pre-Fire		Post-Fire: Flight #1		Post-Fire: Flight #2		
			CC	adjusted CC	CC	Δ1	CC	Δ2	Δ3
Pinet-1	Totally	Yes	48.97%	42.82%	25.53%	-40.39%	26.15%	-38.93%	+2.45%
Pinet-2	Totally	No	52.38%	45.80%	14.45%	-68.44%	No flight		
Pinet-2	Partially	No	48.42%	42.34%	23.82%	-43.73%	No flight		
Pinet-3	Totally	Yes	41.79%	36.54%	26.87%	-26.47%	26.87%	-26.46%	+0.02%
Pinet-4	Totally	No	50.25%	43.94%	29.59%	-32.65%	32.71%	-25.55%	+10.54%
Pinet-5	Unburnt	–	61.28%	53.58%	53.58%	–	No flight		

PFP: Post-fire practices. Δ1: Change in the percentage of canopy cover between the Flight#1 and Pre-fire scenario (adjusted CC). Δ2: Change in the percentage of canopy cover between the Flight#2 and Pre-fire scenario (adjusted CC). Δ3: Change in the percentage of vegetation cover between the Flight#2 and Flight#1 scenarios.

and thus, to refine the assessment of the sole effect of the soil erosion barriers on SC; and (II) because the five sub-sites are located in the same hillslope and geomorphic feature –near the crest– and soils are developed over the same parent material (Cretaceous marble limestones with dolomite layers; see Appendix A).

Index setup includes several conditions. In Eq. (2), slope gradient of less than 0.005 must be adjusted to $S_i = 0.005$ and higher than 1 must be set to a maximum value of $S_i = 1$. The weighted flow path length and upslope factors ($\overline{R}$, $\overline{RT}$, $\overline{C}$, $\overline{K_P}$ and $\overline{S}$) were calculated using the D-Infinity algorithm that bifurcate flow to a maximum of two neighbours. In this study, we did not define any specific computation target because the intersected areas of the five sub-sites do not correspond to the hydrological boundaries of any sub-basin or catchment. Thus, the pixel/s located at the lowest elevation/s of each sub-site acted as the target/s of the simulation, regardless the actual drainage area of that/those pixel/s could be larger if the whole landscape was considered.

AIC outputs depend on the simulation target (type and location) and input resolution (pixel size). Therefore, a two-step output modification was necessary in this study to correct computation differences and to obtain comparable values (see Appendix A):

- *1st modification*. As the drone-flight areas at each sub-site, and the intersected areas, do not match with any hydrological sub-catchment, there are different small sub-basins at each intersected area, and the number and shape of these sub-basins also depend on the cell size. In order to obtain comparable values throughout each sub-site, we corrected the AIC outputs of Eq. (1) by using the following expression proposed by López-Vicente et al. (2021):

$$AIC_{Corr} = AIC_i \times \log_{10}(10 + FlowLength_{sim}) \quad (3)$$

  where AIC_{Corr} is the corrected index of SC. This adjustment was done for each basin separately, using its own flow path length (m) and considering its simulation target (outlet) as a reference.
- 2nd *modification*. Fractal geometry is expected due to the decreasing cell size (IGN- and drone-derived DEMs), thus, adjustment of the AIC distributions improves comparisons between the different AIC maps (López-Vicente and Álvarez, 2018). In this study, we used the unburnt control site (Pinet-5) to compare the maps and values of AIC before and after the fire (first drone flight) and adjusted the AIC_{Corr} values of the two maps. Then, the calculated adjustment coefficient was used to adjust the values of the other sub-sites at the Pre-Fire scenario.

2.5. Statistical analysis and metrics for evaluation

The statistical analysis of the differences between the maps of flow length and sediment connectivity over the three temporal scenarios at each sub-site was done by calculating the ANOVA with Tukey test (95% of confidence) on a random selection of 200 points at each sub-site. The same net was used for all comparisons and was generated using the 'Create Random Points' tool (*ArcGIS Pro*) with a minimum allowed distance of 1 m between points. Additionally, we analysed the spatial distribution of the areas with the highest (above percentile 90 – P90) and lowest (below percentile 10 – P10) values of SC by means of mapping these areas and observing whether the location of these areas remained in the same places or changed over time.

3. Results and discussion

3.1. Vegetation recovery rates

The calculated values of canopy cover (CC; defined as the proportion of the ground forest covered by the vertical projection of the tree and shrub crowns) two months before the fire ranged between 41.8% and 61.3% ($\bar{x}$=50.5%; σ = 7.0%) (Table 3). These values can be considered representative of a Mediterranean forest, such as López-Vicente and Navas (2009) observed in a mountainous semi-arid area in north-eastern Spain –with a similar stony soil as in this study– with CC values ranging between 27.5% (disperse scrubland) and 80.7% (dense forest, including holm oak and pine species). Hernandez-Tecles et al. (2015) also obtained comparable values of CC in pine forests located in a neighbouring province –Albacete– from our study site and under the same rainfall regime in natural ($\bar{x}$=60 ± 3%) and planted ($\bar{x}$=66 ± 3%) stands. Forest and farmlands in the eastern part of Spain are usually developed on stony soils –limestone rocks frequently cover a significant percentage of the ground (Pérez-de-los-Reyes et al., 2020)– like in our study area where the rock coverage ranges between 6.0% and 24.6% ($\bar{x}$=16.3%; σ = 8.5%).

In the first post-fire scenario, CC was of 25.5%, 14.5%, 23.8%, 26.9% and 29.6% in Pinet-1, P-2_totally_burnt_area, P-2_partially_burnt_area, P-3 and P-4, respectively ($\bar{x}$=24.1%; σ = 5.8%), which means an annual average rate of canopy cover recovery –in the four fire-affected sub-sites– of 27.5% per year (σ = 6.6%) (Table 3). These values were obtained after excluding the anthropogenic land uses, such as the unpaved forest roads, and the small building in Pinet-3. Taking into account that the first drone flight was done only 10.5 months after the fire, these CC recovery rates are high, but they totally agree with the recovery ratios calculated by Viana-Soto et al. (2020) in fire-affected woodlands (coniferous forests with certain deciduous species of the genus *Quercus*, and sclerophyll species in the understory) located in Valencia and Albacete provinces, where the recovery of the Tasseled Cap Angle –related to vegetation cover gradients– was high shortly after the fire due to the early post-fire colonization of annual herbs and shrubs. In a South African Mediterranean-type climate area, Rutherford et al. (2011) also found a quick increase in plant CC of herbs in the first year after the fire, whereas the increase in CC of shrubs and graminoids was relatively slow in the first year, but the cover of annual plants increased every year.

In order to properly compare the pre-fire scenario (aerial orthophoto) with the post-fire mosaics –generated with the drone-derived images–, we used the unburnt control area –Pinet-5–. In this sub-site,

Table 4
Mean values and temporal changes (in %) of flow length (FL; m) in the five sub-sites during the three temporal scenarios: Pre-fire (06/2018), Flight-1 (06/2019) and Flight-2 (02/2020). In bold, when differences among scenarios (expressed as Δ1, Δ2, Δ3) are statistically significant.

Sub-site	Burnt degree	PFP	Pre-Fire		Post-Fire: Flight #1		Post-Fire: Flight #2		
			mean	adjusted FL	mean	Δ1	mean	Δ2	Δ3
Pinet-1	Totally	Yes	72.60	92.84	91.61	-1.33% ($p = 0.224$)	100.00	+7.71% ($p = 0.865$)	+9.16% ($p = 0.139$)
Pinet-2	Totally	No	91.44	116.94	90.28	**-22.80% (p=0.009)**	No flight		
Pinet-2	Partially	No	76.65	98.02	79.18	**-19.23% (p=0.042)**	No flight		
Pinet-3	Totally	Yes	92.86	118.75	109.76	-7.57% ($p = 0.568$)	101.58	**-14.46% (p=0.028)**	-7.45% ($p = 0.055$)
Pinet-4	Totally	No	136.36	174.38	174.65	+0.15% ($p = 0.303$)	177.25	+1.64% ($p = 0.497$)	+1.49% ($p = 0.679$)
Pinet-5	Unburnt	–	86.52	110.64	110.64	–	No flight		

PFP: Post-fire practices. Δ1: Change in the mean flow length between the Flight#1 and Pre-fire scenario (adjusted FL). Δ2: Change in the mean flow length between the Flight#2 and Pre-fire scenario (adjusted FL). Δ3: Change in the mean flow length between the Flight#2 and Flight#1 scenarios.

it is expected that CC before and after the fire was roughly the same; however, the differences in images resolution and data sources may affect the assessment of CC. Indeed, the estimated CC in Pinet-5 with the orthophoto was 61.28% and with the first drone flight was 53.58%, which makes a ratio between both values of 0.874. We then used this ratio to modify the obtained values of CC in the four fire-affected sub-sites with the orthophoto, and calculated the differences between the pre-fire and post-fire scenarios (Δ1) with the corrected CC estimates. Values of Δ1 were of −40.4%, −68.4%, −43.7%, −26.5% and −32.7% in Pinet-1, P-2_totally_burnt_area, P-2_partially_burnt_area, P-3 and P-4, respectively. In the totally burnt areas with LEB (Pinet-1 and Pinet-3), the average Δ1 was of −33.43%; whereas Δ1 in the totally burnt areas without LEB (Pinet-2_totally_burnt and Pinet-4) was of −50.55%. In the partially burnt area of Pinet-2, Δ1 has an intermediate value of −43.73%. These results clearly support the effectiveness of LEB to favour vegetation recovery in terms of canopy cover, in spite of the short time period between the fire, the PFP installation and the first drone flight. It is worthy of note that the recovery of CC in the totally burnt area with LEB was higher than in the partially burnt area. Therefore, CC recovery not only depends on fire severity, such as many studies have proven (e.g. Maia et al., 2012), but on the implementation of post-fire practices. Although no statistical analysis could be performed to identify significant differences among treatments due to the limited number of sub-sites, the obtained results of higher CC recovery in the areas with LEB in the first year after the fire were in agreement with the results reported by López-Vicente et al. (2021) in a burnt pine forest in southern Spain, where new vegetation was observed in 24.7% of the slope area with erosion barriers –22 months after the fire–, whereas new vegetation covered 20.0% of the slope without PFP. Lucas-Borja et al. (2021) also found in central-eastern Spain that the initial seedling recruitment of Spanish black pine was improved by contour-felled log debris treatment, specifically through increased survival of emergent seedlings by about 10 times, compared to control. However, Raftoyannis and Spanos (2005) found in a Mediterranean pine forest in Greece that the construction of log and branch barriers was not effective in post-fire ecosystem recovery because the slope orientation affected in a greater way the revegetation process and it was more successful on the north wetter slopes.

In the second post-fire scenario, 18 months after the fire and 13 months after the PFP, CC increased up to 26.2%, 26.9% and 32.7% in Pinet-1, Pinet-3 and Pinet-4, respectively ($\overline{x}$=28.6%; σ = 3.6%), and the annual average rate of CC recovery –in these three sub-sites– was of 19.1% per year (σ = 2.4%) (Table 3). The lower rate of CC recovery in the second post-fire scenario, −31% with respect to the first post-fire scenario, indicated a slowdown of vegetation recovery. The CC increment among the post-fire scenarios (Δ3; 7.5-month time lapse) was of 2.45%, 0.02% and 10.54% in Pinet-1, Pinet-3 and Pinet-4, respectively. Viana-Soto et al. (2020) also found that the recovery ratio of the vegetation varied across the different stages, with decreasing rates after the first stage when the recovery was great. In particular, these authors explained the lower vegetation recovery of the subsequent stages in a young regrowth forest because of the intense competition among regenerated species. Drought stress can play an important role in the vegetation recovery rate in Mediterranean-type climatic areas, such as Hope et al. (2007) underscored after characterizing post-fire vegetation recovery of California chaparral using satellite imagery. In our case, the total rainfall depth in the first 10.5 months after the fire (from 13 August 2018 till 27 June 2019: 1049.2 mm) was 36% higher than the 10-yr pre-fire average value during the same period (from August of year 'x' to June of the year 'x + 1': 770.4 mm). During the period between the first and the second drone flight (from 28 June 2019 till 3 February 2020: 1140.6 mm), the total rainfall depth was 122% higher than the 10-yr pre-fire average value during the same period (from July of year 'x' to January of year 'x + 1': 514.3 mm) (data source: Júcar River-Basin Authority – SAIH-CHJ, weather station "Pinet (9P03)"). These values of precipitation could partially explain the rapid CC recovery during the first 10.5 months after the fire, due to humid conditions than the average, and at the same time highlight the rapid decrease in the CC recovery rate during the second year after the fire despite the very humid conditions during that period.

Regarding the effectiveness of the LEB eighteen months after the fire, the two totally burnt sub-sites with LEB (Pinet-1 and Pinet-3) had an average Δ2 of −32.69%; whereas Δ2 in Pinet-4 (totally burnt area without LEB) was of −25.55%. These results modulated those obtained in the first year after the fire, suggesting a faster CC recovery in the sub-sites with LEB in the first year, but faster CC recovery in the second year in the sub-site without LEB. Fernández et al. (2011) also found in north-western Spain –under more humid conditions than those in Pinet– that vegetation regrowth was very fast during the first two years after the wildfire, and the different evaluated treatments (straw mulch, wood-chip mulch, cut-shrub barriers and control) had no significant effect on the rate of recovery of vegetation cover. Another consideration is that the estimated CC recovery rates in a landscape with different plant species cannot be directly extrapolated to the biomass recovery, because the relationship between CC and above-ground biomass (AGB) ranges between potential approaches for short plants (Jia et al., 2014) to linear approaches for tall woody species (Brūmelis et al., 2020). Besides, the relationship between canopy area and tree height is potential (Ansley et al., 2012), and that between canopy height and AGB is in between linear and potential (Köhler and Huth, 2010). Indeed, Rodrigues et al. (2014) calculated that the total-recovery time of plant communities after high-severity wildfires in Spain ranges between 2 and approximately 100 years for grassland and woodland with low germination, respectively. Therefore, further studies should consider the assessment of the 3D structure of the new vegetation in order to obtain a better estimation of the actual vegetation recovery rates.

3.2. Sediment connectivity changes

Flow length (FL; m) –included in the downslope module ($\boldsymbol{D_{dn}}$) of AIC, and expressed as $\sum_{k=i}^{n} d_i$– changed over the temporal scenarios, and the magnitude of this change differed between the five sub-sites (Table 4).

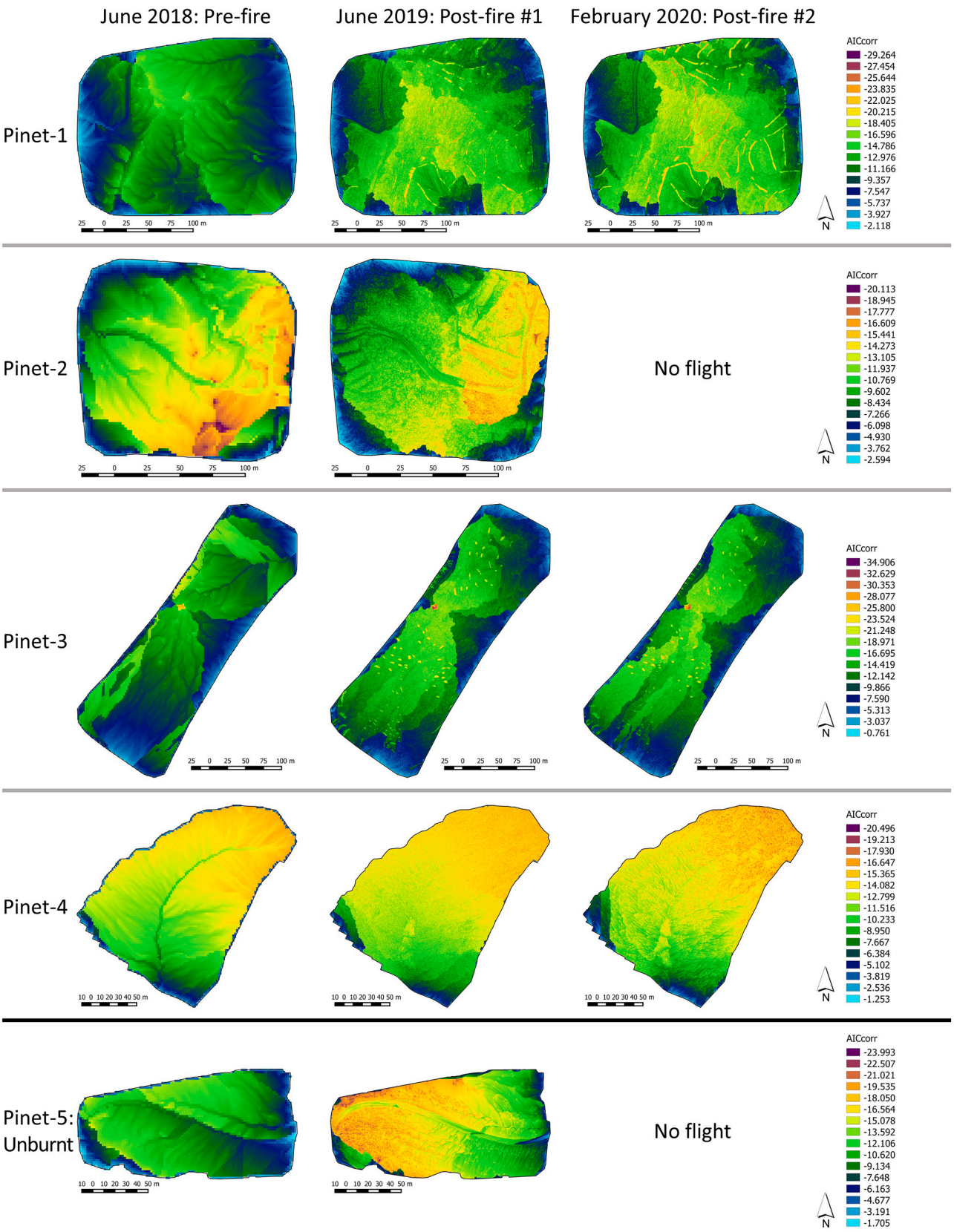

Fig. 5. Maps of sediment connectivity estimated with the AICv2 and expressed as AIC_{Corr}.

Table 5
Mean values and temporal changes (in %) of the aggregated index of connectivity (AIC_{Corr}) obtained in the five sub-sites during the three temporal scenarios: Pre-fire (06/2018), Flight-1 (06/2019) and Flight-2 (02/2020). In bold, when differences among scenarios (expressed as Δ1, Δ2, Δ3) are statistically significant.

Sub-site	Burnt degree	PFP	Pre-Fire		Post-Fire: Flight #1		Post-Fire: Flight #2		
			mean	adjusted AIC_{Corr}	mean	Δ1	mean	Δ2	Δ3
Pinet-1	Totally	Yes	-10.415	-15.738	-12.882	**+18.15% ($p<0.001$)**	-13.426	**+14.69% ($p<0.001$)**	-4.23% ($p = 0.113$)
Pinet-2	Totally	No	-12.206	-18.444	-10.728	**+41.84% ($p<0.001$)**	No flight		
Pinet-2	Partially	No	-11.461	-17.318	-10.731	**+38.04% ($p<0.001$)**	No flight		
Pinet-3	Totally	Yes	-11.341	-17.137	-12.541	**+26.82% ($p<0.001$)**	-12.575	**+26.62% ($p<0.001$)**	-0.28% ($p = 0.711$)
Pinet-4	Totally	No	-11.975	-18.095	-12.635	**+30.18% ($p<0.001$)**	-12.639	**+30.15% ($p<0.001$)**	-0.04% ($p = 0.922$)
Pinet-5	Unburnt	–	-9.717	-14.684	-14.684	–	No flight		

PFP: Post-fire practices. Δ1: Change in the mean value of AIC_{Corr} between the Flight#1 and Pre-fire scenario (adjusted AIC_{Corr}). Δ2: Change in the mean value of AIC_{Corr} between the Flight#2 and Pre-fire scenario (adjusted AIC_{Corr}). Δ3: Change in the mean value of AIC_{Corr} between the Flight#2 and Flight#1 scenarios.

To obtain comparable values over the studied period, and taking into account the different topographic data sources (from IGN and the drone flights), we used the two DEMs of the unburnt control sub-site (Pinet-5) to calculate a correction coefficient, in order to have the same FL in this sub-site before and after the fire. After correcting the FL pre-fire values and compared with the pre-fire scenario, the changes in the average FL ($\overline{FL}$) obtained in the first drone flight (Δ1; %) differed among the different sub-sites, namely: −1.3% in the sub-site with long LEBs, −7.6% in the sub-site with short LEBs, −11.3% in the totally burnt areas without LEBs, and −19.2% in the partially burnt area without LEBs. In the second drone flight, the differences with the pre-fire scenario (Δ2; %) in the three sub-sites with data, were more changeable and no clear trend was observed. However, the differences between the two drone flights (Δ3; %) showed that $\overline{FL}$ increased in both the sub-sites with (+0.9%) and without LEBs (+1.5%). This fact may be explained by the incipient breakdown of the LEBs that could affect the surface area covered by the cut trunks and branches, such as Robichaud et al. (2008) observed in southern California where degradation over time reduced the effectiveness of contour-felled log erosion barriers. The temporal changes obtained with Δ1, Δ2 and Δ3 were only significant ($p < 0.05$) in three of the eleven cases (Table 4).

In general, these results indicated that not installing LEBs favoured much shorter flow length pathways after the fire for a specific area, and thus, runoff will flow faster to cover the same surface, achieving higher velocity, and thus, soil detachment capacity and sediment concentration could be expected to be higher. These results agree with those reported by Robichaud et al. (2020) who observed higher runoff velocity in control and scarified plots (located in Colorado State, USA) over different post-fire years and compared with plots that included post-fire management measures. In steep slopes with shrub-dominated vegetation, and under continental climate conditions, Pierson et al. (2009) also found that removal of vegetation and ground cover facilitated increased runoff velocity and transport capacity of overland flow compared with unburnt control areas.

In the pre-fire scenario, the maps of sediment connectivity showed different spatial patterns among the sub-sites associated with the presence of forest trails (Pinet-1, Pinet-2, Pinet-3 and Pinet-5), numerous (Pinet-1, Pinet-2 and Pinet-3), moderate (Pinet-5) or reduced (Pinet-4) number of small sub-basins, and the high heterogeneity (Pinet-1 and Pinet-2), moderate heterogeneity (Pinet-3 and Pinet-5), or low heterogeneity (Pinet-4) in the land uses (Fig. 5). As expected, forest trails and those land uses with lower values of ground cover presented the higher AIC values, in agreement with other studies of soil erosion and sediment connectivity in Mediterranean forests (e.g. López-Vicente et al., 2020; Salesa and Cerdà, 2020).

In the two post-fire scenarios, the effect of the LEBs appeared markedly in the maps of sediment connectivity, modifying both the spatial patterns and the values of AIC (Fig. 5) (Table 5). In the four burnt sub-sites and based on the pre-fire scenario, sediment connectivity increased in the two post-fire scenarios. However, changes in connectivity differed among the sub-sites, appearing the lowest increments in the two sub-sites with presence of LEBs ($\overline{\Delta 1}$=+22.5%), and higher and similar increments in the sub-sites without LEBs and with areas totally ($\overline{\Delta 1}$=+36.0%) and partially ($\overline{\Delta 1}$=+38.0%) burnt. In general, the observed increment of sediment connectivity ranged in a similar way as other increments of sediment delivery measured in fire-affected areas, such as in the island of Mallorca (Spain) (García-Comendador et al., 2017) and in Colorado (USA) (Wilson et al., 2021), where field-measured sediment yield increased significantly after the fire, but the magnitude of the change depended on the intensity of the rainfall event. Therefore, further research in Pinet should include functional sediment connectivity that will complement the current study of structural connectivity. In particular, the different changes in connectivity due to the presence of LEBs agreed with the overall conclusions reported in a recent review about the effectiveness of post-fire soil erosion mitigation treatments (Girona-García et al., 2021). In this study, authors concluded that the application of the mitigation treatments represented a better choice than doing nothing, especially in sites where soil erosion is high, and the effectiveness of the treatments was greatest shortly after the fire.

Between the two post-fire scenarios, sediment connectivity decreased in all burnt sub-sites, ranging this reduction between −0.04% and −4.23%, because of the higher values of canopy cover in the second post-fire scenario with regard to the first post-fire scenario. This small reduction of connectivity agreed with the results obtained in an 11-year study of soil loss dynamics during vegetation recovery in fire-affected areas in South Korea (Kim et al., 2021). These authors found that soil stabilization took between 3 and 7 years depending on the initial vegetation cover conditions. Regarding the two types of LEBs, the increment of sediment connectivity during the first and second post-fire scenarios, and based on the pre-fire scenario, was 32% and 45% lower in the sub-site with long LEBs than the increment observed in the sub-site with short LEBs, highlighting the greater efficiency of the long LEBs.

In order to evaluate the spatial distribution of the AIC changes, the areas with the highest (above percentile 90 – P90) and lowest (below percentile 10 – P10) values of AIC were mapped, observing whether the location of these areas remained in the same places or changed over time (Fig. 6). The areas with the highest AIC values did not change over the three temporal scenarios, owing to their spatial location, near the multiple outlets of each sub-site, and far from the areas with LEBs. However, clear and marked changes appeared in the location of the areas with the lowest values of sediment connectivity (P10) in the two sub-sites with LEBs (Pinet-1 and Pinet-3). In these two sub-sites, the P10 pixels were mainly located in the same places where LEBs were installed and in their surrounding areas. In the control unburnt area (Pinet-5) and the two subsites without LEBs (Pinet-2 and Pinet-4), the location of the P10 pixels did not differ greatly over the scenarios. These results stress the usefulness of the LEBs to create areas with very low sediment transport capacity. The results of Gómez-Sánchez et al. (2019) –obtained with plots in a Spanish similar area of this study– also revealed the efficacy of LEBs and contour-felled log debris in retaining sediments and limiting loss of nutrients, which is considered essential to recover vegetation

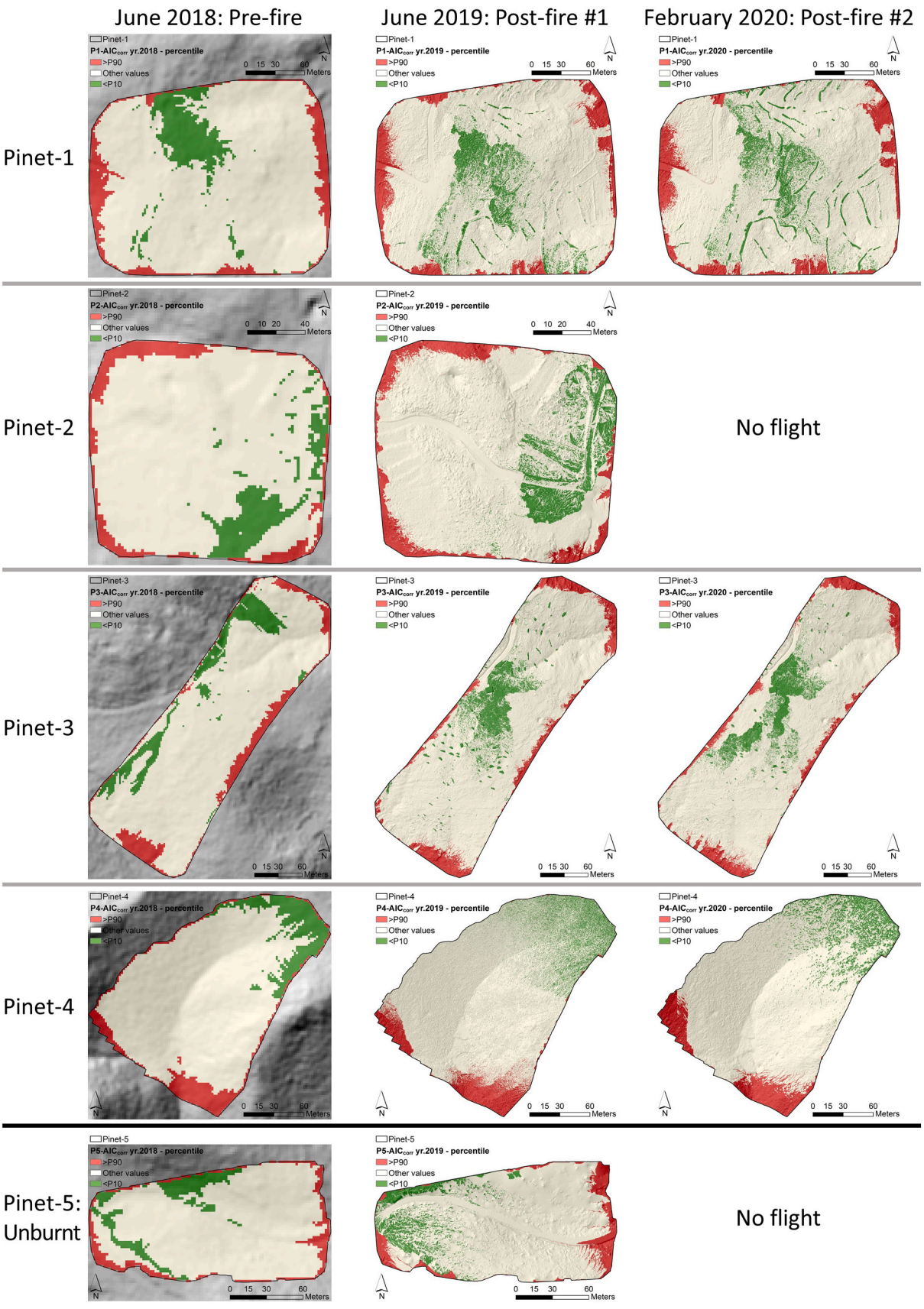

Fig. 6. Maps of the areas with the highest (above percentile 90) and lowest (below percentile 10) values of sediment connectivity estimated with the AICv2 in the five sub-sites and over the three studied years.

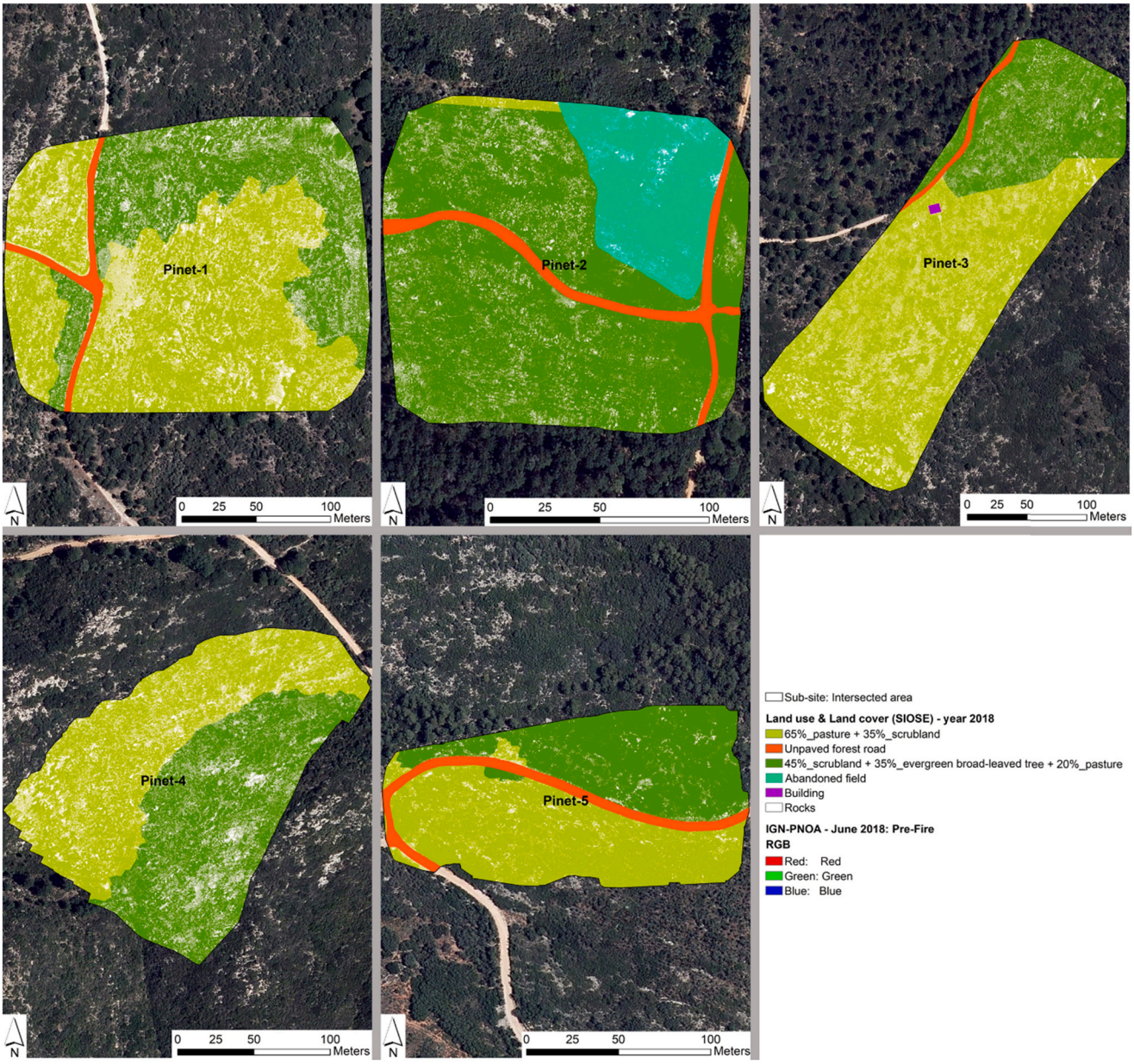

Fig. A1. Map of land use and land cover in June 2018, two months before the fire.

after a wildfire.

3.3. Implications for better post-fires practices

It is worth noting the difference response of sediment connectivity between the short and long barriers. Long log-erosion barriers clearly promoted the dis-connectivity just upslope from the barriers, which can favour the infiltration of runoff and withholds water, nutrients and sediment on this location, favouring vegetation growth. However, the vegetation recovery in the untreated sub-sites was better when comparing the first and second drone flights. Furthermore, in the treated areas there will be always the area with the logs that will not have any vegetation until the total decomposition of the burnt trees and branches. In Mediterranean-type ecosystems, the rate of wood decomposition (loss of density) after fires ranges from an average 11% at the highest-elevation areas to 32% at an intermediate elevation (Molinas-González et al., 2017).

In this study, all forest trails already exist before the fire, and thus, the impact of trails on vegetation recovery and sediment connectivity could not be evaluated. Further research in other areas with new skid trails remains necessary in order to calculate the trade-off between promoting of vegetation and reduction of runoff and erosion near the barriers, but enhancing the runoff on skidding trails. Finally, a study focus on the native palm should be done to calculate the specific vegetation recovery rate per plant species.

Another key issue that should be researched in the near future is how the trampling of workers and the passes of machinery that build barriers and other post-fire restoration and rehabilitation strategies will affect soil properties and plant recovery (Kissling et al., 2009). This research should shed light on the runoff generation and sediment yield from a long-term point of view. This is because the recovery of the vegetation along the first and second year after the fire found in Pinet is only the beginning of a long process of ecosystem recovery. Trampling can result in a more compacted soil that will contribute with more runoff such as it is found in areas affected by grazing (Savadogo et al., 2007). Another key issue is the use of machinery that can induce changes in the soil

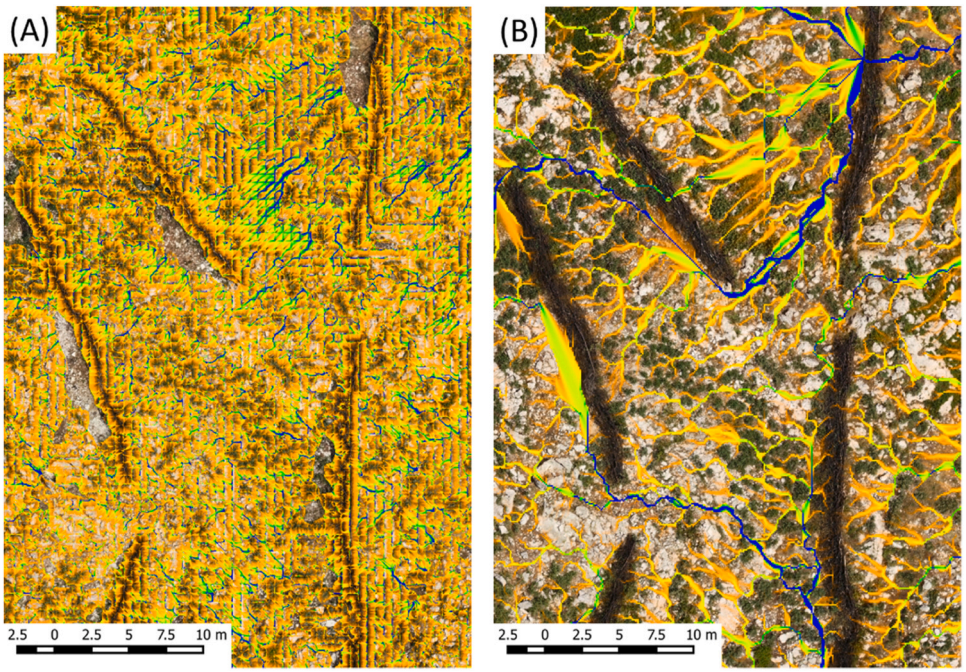

Fig. A2. Overland flow pattern in Pinet-1, in 2019, obtained with the resample DEM at 5 × 5 cm (A) and 10 × 10 cm (B) of pixel size.

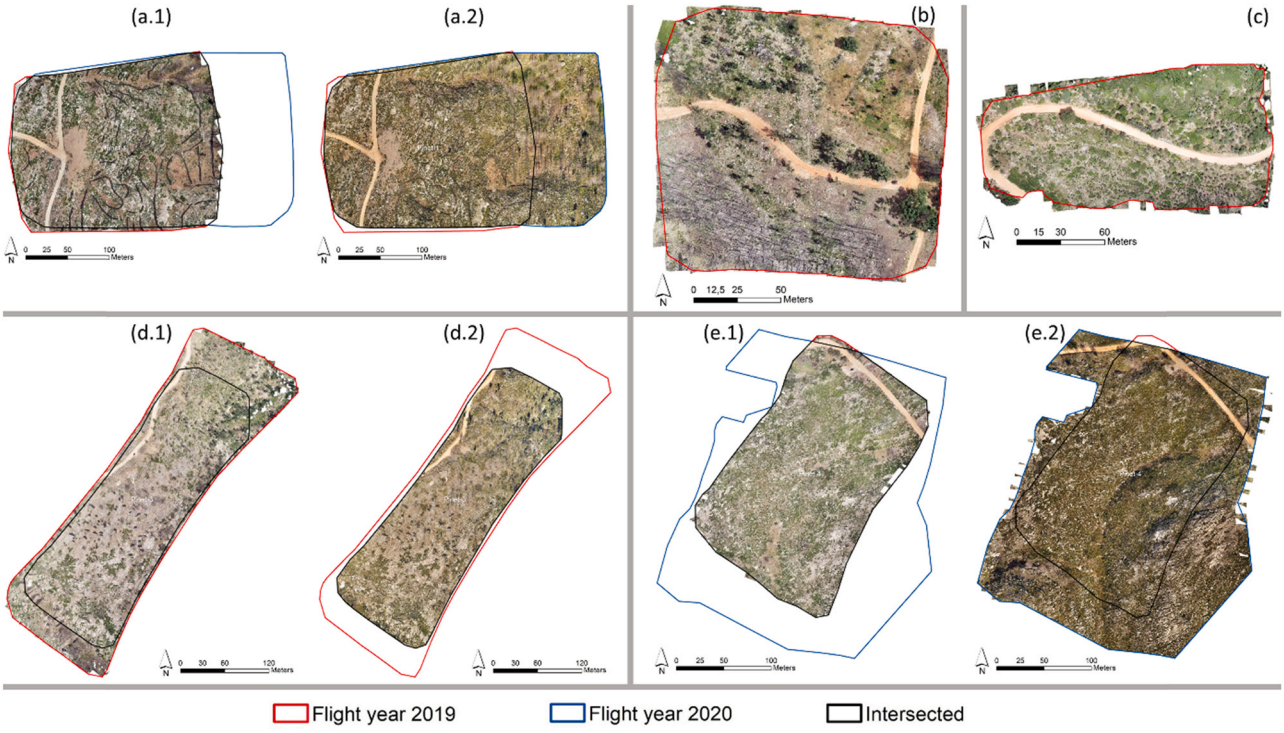

Fig. A3. Orthomosaics of the five sub-sites generated with the images taken during the two drone flights in: Pinet-1 (a.1 and a.2), Pinet-2 (b), Pinet-5 (c), Pinet-3 (d.1 and d.2) and Pinet-4 (e.1 and e.2). The intersected area between the two flights at each sub-site is also presented, except in Pinet-2 and Pinet-5 where only one flight was done at each sub-site.

system that will result in the degradation of soil properties and as a consequence on higher soil erosion rates. This will be depend on the type and use of machines. Fernández-Moya et al. (2014) and Picchio et al. (2012) already found that the impact of machinery on soils and on vegetation recovery needs more investigation. Moreover, changes in the soil properties after forest fires last for years, or even decades. This means, that changes in connectivity can be sudden due to the forest fire, due to the plant cover recovery in the first year, but also can last longer due to changes in the soil properties such as soil water repellency (Li et al., 2021). After forest fires, the reduction in the soil water repellency degree will enhance infiltration, but later the process is reversed. The merging of data about vegetation recovery, soil physical and chemical properties, and sediment dynamic will lead to a better understanding of the soil health status at local scale and ecosystem services at landscape

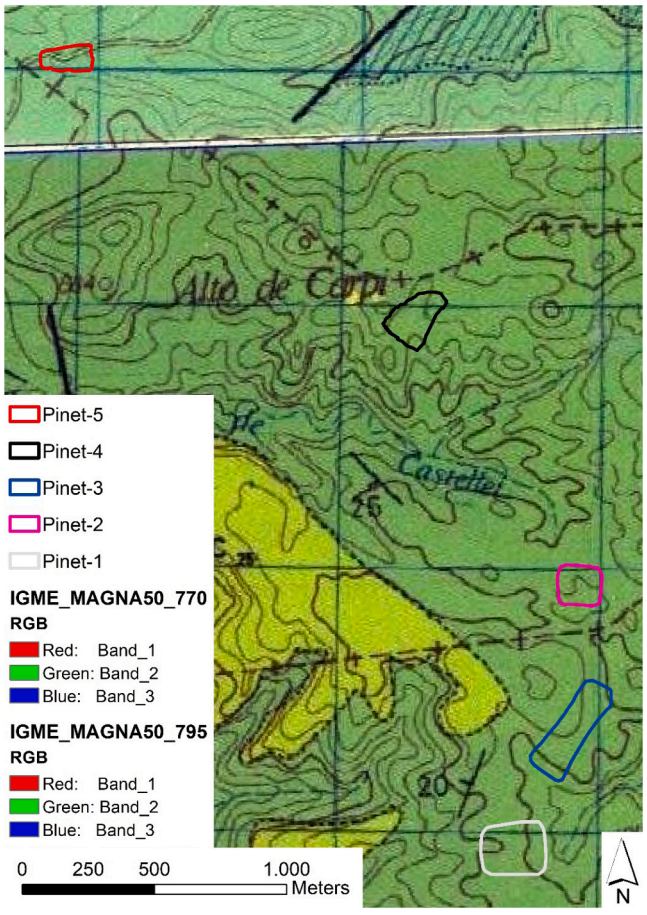

Fig. A4. Geological map of the study area showing the boundary of the five sub-sites.
Data source: Spanish Geological Survey – IGME.

scale (Keesstra et al., 2021). Future studies will contribute to a more accurate information to understand the connectivity issue in fire affected land, with special attention to fire-dependent ecosystems where we need to advance in the development of ecosystem management strategies that work with, not against, fire (Pivello et al., 2021). For example, we found that the recovery in the second post-fire year was better in the non-treated areas, which is probably due to the lack of trampling of workers and the past of machinery as restoration works did not take place. However, this research needs a field-based scientific approach to determine how much and how long the post-fire treatments affect in a positive or negative way the ecosystem's recovery.

Table B1
Assigned C-factors at the 25 land covers identified in the five sub-sites and over the three temporal scenarios.

Land use	Sub-site	C-factor		
		2018	2019	2020
(45%Scrubland+35% EvergreenBroadLeavedTree+20% PST)	P1	0.0224	ND	ND
(45%Scrubland+35% EvergreenBroadLeavedTree+20% PST)	P2	0.0230	ND	ND
(45%Scrubland+35% EvergreenBroadLeavedTree+20% PST)	P3	0.0272	ND	ND
(45%Scrubland+35% EvergreenBroadLeavedTree+20% PST)	P4	0.0255	ND	ND
(45%Scrubland+35% EvergreenBroadLeavedTree+20% PST)	P5	0.0178	0.0156	ND
(35%Scrubland+65%PST)	P1	0.0692	ND	ND
(35%Scrubland+65%PST)	P2	0.0572	ND	ND
(35%Scrubland+65%PST)	P3	0.0750	ND	ND
(35%Scrubland+65%PST)	P4	0.0589	ND	ND
(35%Scrubland+65%PST)	P5	0.0544	0.0591	ND
Abandoned field	P2	0.0881	ND	ND
Unpaved forest road	P1-P5	0.5027	0.5027	0.5027
Building	P3	0.0001[a]	0.0001[a]	0.0001[a]
Rocks	P1-P5	0.0001[a]	0.0001[a]	0.0001[a]
Log-erosion barrier	P1, P3	ND	0.0010	0.0010
Totally burnt	P1	ND	0.3457	0.3373
Totally burnt	P2	ND	0.4931	ND
Totally burnt	P3	ND	0.3278	0.3277
Totally burnt	P4	ND	0.2916	0.2501
Partially burnt	P2	ND	0.3683	ND

[a]We used this value, instead of zero, to avoid any computational error with the *ArcGIS* tools.

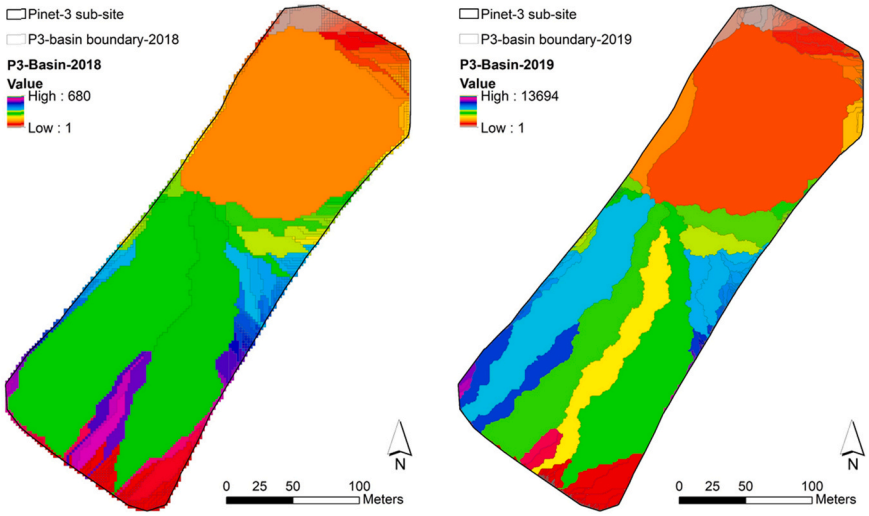

Fig. A5. Number and shape of the small sub-basins in Pinet-3 obtained with the DEMs of the years 2018 and 2019.

4. Conclusions

The use of drone-derived images has allowed an accurate estimation of the post-fire vegetation recovery rates in a Mediterranean landscape with rock-outcrop and stony soils, and rolling topography. Overall, the results of canopy cover changes of the two post-fire scenarios indicate that (I) in the treated areas with log-erosion barriers, the recovery was quite stable and quick during the first post-fire year; (II) in the non-treated areas, the responses were contrasted, with positive changes in some areas and negatives in others; and (III) the recovery in the second post-fire year was better in the non-treated areas. These results have to be evaluated with caution because all post-fire scenarios show the effect of the fire plus the post-fire management and the intrinsic physiographic differences among the sub-sites. Further research should include the effect of fire on ground conditions that could affect plant sprout and growth. In addition, the results of this study may be influenced by the Mediterranean vegetation type and climatic conditions of the study area, and thus, further research under distinct edaphic conditions and biomes is necessary to allow sound conclusions. Regarding overland flow processes, log-erosion barriers effectively lengthened overland flow pathways, reducing runoff detachment capacity, and reduced sediment connectivity in the first post-fire year, but their usefulness was not as pronounced during the second post-fire year. Why is this is probably a result of the trampling and machinery passes that should be further studied by means of laboratory and field approaches.

CRediT authorship contribution statement

Manuel López-Vicente and Saskia Keesstra conceived of the present study and developed the theory. Manuel López-Vicente, Artemi Cerdà and Saskia Keesstra wrote the manuscript. Manuel López-Vicente and Henk Kramer performed the computations. All authors verified the analytical methods, supervised the findings of this work, discussed the results and contributed to the final manuscript.

Acknowledgements

This research was funded by the project SPECTORS, which is a Dutch-German cooperation project funded by INTERREG V-A Deutschland-Nederland. This research was also included in the research activities of the European COST Action FIRElinks (CA18135) “Fire in the Earth System: Science & Society” (European Union Framework Programme Horizon 2020). This research was also partially funded by the Netherlands Ministry of Agriculture, Nature and Food Quality (grant number KB-36–005-006/008; Nature-inclusive Transitions).

Appendix A. Maps used to characterize the study area and for configuring the index of connectivity

(see Figs. A1-A5).

Appendix B. Table used for configuring the index of connectivity

(see Table B1).

Appendix C. Supporting information

Supplementary data associated with this article can be found in the online version at doi:10.1016/j.landusepol.2021.105776.

References

Albert-Belda, E., Bermejo-Fernández, A., Cerdà, A., Taguas, E.V., 2019. The use of Easy-Barriers to control soil and water losses in fire-affected land in Quesada, Andalusia, Spain. Sci. Total Environ. 690, 480–491. https://doi.org/10.1016/j.scitotenv.2019.06.303.

Alloza, J.A., Santana, V.M., Valdecantos, A., Vallejo, V.R., 2018, Informe sobre el impacto del incendio forestal de Llutxent, 2018. CEAM (Fundación Centro de Estudios Ambientales del Mediterráneo). Paterna, Valencia, Spain. ⟨http://www.ceam.es/GVAceam/archivos/INFORME_Incendio_luxent_2018.pdf⟩.

Ansley, R.J., Mirik, M., Surber, B.W., Park, S.C., 2012. Canopy area and aboveground mass of individual Redberry Juniper (Juniperus pinchotii) trees. Rangel. Ecol. Manag. 65 (2), 189–195. https://doi.org/10.2111/REM-D-11-00112.1.

Badía, D., Sánchez, C., Aznar, J.M., Martí, C., 2015. Post-fire hillslope log debris dams for runoff and erosion mitigation in the semiarid Ebro Basin. Geoderma 237, 298–307. https://doi.org/10.1016/j.geoderma.2014.09.004.

Beghin, R., Lingua, E., Garbarino, M., Lonati, M., Bovio, G., Motta, R., Marzano, R., 2010. Pinus sylvestris forest regeneration under different post-fire restoration practices in the northwestern Italian Alps. Ecol. Eng. 36 (10), 1365–1372. https://doi.org/10.1016/j.ecoleng.2010.06.014.

Bonazountas, M., Kallidromitou, D., Kassomenos, P., Passas, N., 2007. A decision support system for managing forest fire casualties. J. Environ. Manag. 84 (4), 412–418. https://doi.org/10.1016/j.jenvman.2006.06.016.

Brūmelis, G., Dauškane, I., Elferts, D., Strode, L., Krama, T., Krams, I., 2020. Estimates of tree canopy closure and basal area as proxies for tree crown volume at a stand scale. Forests 11, 1180. https://doi.org/10.3390/f11111180.

Budde, K.B., González-Martínez, S.C., Navascués, M., Burgarella, C., Mosca, E., Lorenzo, Z., Zabal-Aguirre, M., Vendramin, G.G., Verdú, M., Pausas, J.G., Heuertz, M., 2017. Increased fire frequency promotes stronger spatial genetic structure and natural selection at regional and local scales in Pinus halepensis Mill. Ann. Bot. 119 (6), 1061–1072. https://doi.org/10.1093/aob/mcw286.

Calama, R., Manso, R., Lucas-Borja, M.E., Espelta, J.M., Piqué, M., Bravo, F., del Peso, C., Pardos, M., 2017. Natural regeneration in Iberian pines: a review of dynamic processes and proposals for management. For. Syst. 26 (2), eR02S. https://doi.org/10.5424/fs/2017262-11255.

Cavalli, M., Vericat, D., Pereira, P., 2019. Mapping water and sediment connectivity (Editorial). Sci. Total Environ. 673, 763–767. https://doi.org/10.1016/j.scitotenv.2019.04.071.

Cerdà, A., Lucas-Borja, M.E., Úbeda, X., Martínez-Murillo, J.F., Keesstra, S., 2017. Pinus halepensis M. versus Quercus ilex subsp. Rotundifolia L. runoff and soil erosion at pedon scale under natural rainfall in Eastern Spain three decades after a forest fire. For. Ecol. Manag. 400, 447–456. https://doi.org/10.1016/j.foreco.2017.06.038.

CLC, 2016, CORINE Land Cover 2006 raster data (Last update May 04, 2021). Available at: ⟨https://www.eea.europa.eu/data-and-maps/data/clc-2006-raster-4⟩ (accessed 13 May 2021).

Diakakis, M., Xanthopoulos, G., Gregos, L., 2016. Analysis of forest fire fatalities in Greece: 1977–2013. Int. J. Wildland Fire 25 (7), 797–809. https://doi.org/10.1071/WF15198.

Ebel, B.A., Moody, J.A., 2017. Synthesis of soil-hydraulic properties and infiltration timescales in wildfire-affected soils. Hydrol. Process. 31 (2), 324–340. https://doi.org/10.1002/hyp.10998.

Van Eck, C.M., Nunes, J.P., Vieira, D.C.S., Keesstra, S., Keizer, J.J., 2016. Physically-based modelling of the post-fire runoff response of a forest catchment in Central Portugal: using field versus remote sensing based estimates of vegetation recovery. Land Degrad. Dev. 27, 1535–1544. https://doi.org/10.1002/ldr.2507.

Elia, M., Giannico, V., Spano, G., Lafortezza, R., Sanesi, G., 2020. Likelihood and frequency of recurrent fire ignitions in highly urbanised Mediterranean landscapes. Int. J. Wildland Fire 29 (2), 120–131. https://doi.org/10.1071/WF19070.

Ellett, N.G., Pierce, J.L., Glenn, N.F., 2019. Partitioned by process: measuring post-fire debris-flow and rill erosion with Structure from Motion photogrammetry. Earth Surf. Process. Landf. 44 (15), 3128–3146. https://doi.org/10.1002/esp.4728.

Fernández-Moya, J., Alvarado, A., Forsythe, W., Ramírez, L., Algeet-Abarquero, N., Marchamalo-Sacristán, M., 2014. Soil erosion under teak (Tectona grandis L.f.) plantations: General patterns, assumptions and controversies. Catena 123, 236–242. https://doi.org/10.1016/j.catena.2014.08.010.

Fernández, C., Fontúrbel, T., Vega, J.A., 2019a. Wildfire burned soil organic horizon contribution to runoff and infiltration in a Pinus pinaster forest soil. J. For. Res. 24 (2), 86–92. https://doi.org/10.1080/13416979.2019.1572091.

Fernández, C., Fontúrbel, T., Vega, J.A., 2019b. Effects of pre-fire site preparation and post-fire erosion barriers on soil erosion after a wildfire in NW Spain. Catena 172, 691–698. https://doi.org/10.1016/j.catena.2018.09.038.

Fernández, C., Vega, J.A., Jiménez, E., Fonturbel, T., 2011. Effectiveness of three post-fire treatments at reducing soil erosion in Galicia (NW Spain). Int. J. Wildland Fire 20 (1), 104–114. https://doi.org/10.1071/WF09010.

de Figueiredo, T., Fonseca, F., Lima, E., Fleischfresser, L., Hernandez, Z., 2017. Assessing performance of post-fire hillslope erosion control measures designed for different implementation scenarios in NE Portugal: Simulations applying USLE (Book Chapter). Wildfires: Perspectives, Issues and Challenges of the 21st Century. Publisher: Nova Science Publishers, Inc, pp. 201–228. ISBN: 978-153612891-8.

Francos, M., Úbeda, X., Tort, J., Panareda, J.M., Cerdà, A., 2016. The role of forest fire severity on vegetation recovery after 18 years. Implications for forest management of Quercus suber L. in Iberian Peninsula. Glob. Planet. Change 145, 11–16. https://doi.org/10.1016/j.gloplacha.2016.07.016.

García-Comendador, J., Fortesa, J., Calsamiglia, A., Calvo-Cases, A., Estrany, J., 2017. Post-fire hydrological response and suspended sediment transport of a terraced Mediterranean catchment. Earth Surf. Process. Landf. 42 (14), 2254–2265. https://doi.org/10.1002/esp.4181.

Girona-García, A., Vieira, D.C.S., Silva, J., Fernández, C., Robichaud, P.R., Keizer, J.J., 2021. Effectiveness of post-fire soil erosion mitigation treatments: a systematic review and meta-analysis. Earth-Sci. Rev. 217, 103611 https://doi.org/10.1016/j.earscirev.2021.103611.

Gómez-Sánchez, E., Lucas-Borja, M.E., Plaza-Álvarez, P.A., González-Romero, J., Sagra, J., Moya, D., De Las Heras, J., 2019. Effects of post-fire hillslope stabilisation techniques on chemical, physico-chemical and microbiological soil properties in Mediterranean forest ecosystems. J. Environ. Manag. 246, 229–238. https://doi.org/10.1016/j.jenvman.2019.05.150.

González-Romero, J., López-Vicente, M., Gómez-Sánchez, E., Peña-Molina, E., Galletero, P., Plaza-Alvarez, P., Moya, D., De las Heras, J., Lucas-Borja, M.E., 2021. Post-fire management effects on sediment (dis)connectivity in Mediterranean forest ecosystems: channel and catchment response. Earth Surf. Process. Landf. esp.5202. https://doi.org/10.1002/esp.5202.

Hernandez-Tecles, E., Osem, Y., Alfaro-Sanchez, R., de las Heras, J., 2015. Vegetation structure of planted versus natural Aleppo pine stands along a climatic gradient in Spain. Ann. For. Sci. 72, 641–650. https://doi.org/10.1007/s13595-015-0490-9.

Hope, A., Tague, C., Clark, R., 2007. Characterizing post-fire vegetation recovery of California chaparral using TM/ETM+ time-series data. Int. J. Remote Sens. 28 (6), 1339–1354. https://doi.org/10.1080/01431160600908924.

Jia, B., He, H., Ma, F., Diao, M., Jiang, G., Zheng, Z., Cui, J., Fan, H., 2014. Use of a digital camera to monitor the growth and nitrogen status of cotton. TheScientificWorldJournal 2014, 602647. https://doi.org/10.1155/2014/602647.

Jiménez-Morillo, N.T., Spangenberg, J.E., Miller, A.Z., Jordán, A., Zavala, L.M., González-Vila, F.J., González-Pérez, J.A., 2017. Wildfire effects on lipid composition and hydrophobicity of bulk soil and soil size fractions under Quercus suber cover (SW-Spain). Environ. Res. 159, 394–405. https://doi.org/10.1016/j.envres.2017.08.022.

Jucker Riva, M., Daliakopoulos, I.N., Eckert, S., Hodel, E., Liniger, H., 2017. Assessment of land degradation in Mediterranean forests and grazing lands using a landscape unit approach and the normalized difference vegetation index. Appl. Geogr. 86, 8–21. https://doi.org/10.1016/j.apgeog.2017.06.017.

Keesstra, S., Sannigrahi, S., López-Vicente, M., Pulido, M., Novara, A., Visser, S., Kalantari, Z., 2021. The role of soils in regulation and provision of blue and green water. Philos. Trans. R. Soc. Lond. Ser. B, Biol. Sci. 376 (1834), 20200175 https://doi.org/10.1098/rstb.2020.0175.

Keesstra, S., Wittenberg, L., Maroulis, J., Sambalino, F., Malkinson, D., Cerdà, A., Pereira, P., 2017. The influence of fire history, plant species and post-fire management on soil water repellency in a Mediterranean catchment: The Mount Carmel range, Israel. Catena 149, 857–866. https://doi.org/10.1016/j.catena.2016.04.006.

Kim, Y., Kim, C.-G., Lee, K.S., Choung, Y., 2021. Effects of post-fire vegetation recovery on soil erosion in vulnerable montane regions in a monsoon climate: a decade of monitoring. J. Plant Biol. 64, 123–133. https://doi.org/10.1007/s12374-020-09283-1.

Kissling, M., Hegetschweiler, K.T., Rusterholz, H.P., Baur, B., 2009. Short-term and long-term effects of human trampling on above-ground vegetation, soil density, soil organic matter and soil microbial processes in suburban beech forests. Appl. Soil Ecol. 42 (3), 303–314. https://doi.org/10.1016/j.apsoil.2009.05.008.

Köhler, P., Huth, A., 2010. Towards ground-truthing of spaceborne estimates of above-ground life biomass and leaf area index in tropical rain forests. Biogeosciences 7, 2531–2543. https://doi.org/10.5194/bg-7-2531-2010.

Laushman, K.M., Munson, S.M., Villarreal, M.L., 2020. Wildfire risk and hazardous fuel reduction treatments along the US-Mexico Border: a review of the science (1986-2019). Air, Soil Water Res. 13, 1–7 https://doi.org/10.1177%2F1178622120950272.

Li, Q., Ahn, S., Kim, T., Im, S., 2021. Post-fire impacts of vegetation burning on soil properties and water repellency in a pine forest. South Korea For. 12 (6), 708. https://doi.org/10.3390/f12060708.

Lopez Ortiz, M.J., Marcey, T., Lucash, M.S., Hibbs, D., Shatford, J.P.A., Thompson, J.R., 2019. Post-fire management affects species composition but not Douglas-fir regeneration in the Klamath Mountains. For. Ecol. Manag. 432, 1030–1040. https://doi.org/10.1016/j.foreco.2018.10.030.

López-Vicente, M., Álvarez, S., 2018. Influence of DEM resolution on modelling hydrological connectivity in a complex agricultural catchment with woody crops. Earth Surf. Process. Landf. 43 (7), 1403–1415. https://doi.org/10.1002/esp.4321.

López-Vicente, M., Ben-Salem, N., 2019. Computing structural and functional flow and sediment connectivity with a new aggregated index: a case study in a large Mediterranean catchment. Sci. Total Environ. 651, 179–191. https://doi.org/10.1016/j.scitotenv.2018.09.170.

López-Vicente, M., González-Romero, J., Lucas-Borja, M.E., 2020. Forest fire effects on sediment connectivity in headwater sub-catchments: evaluation of indices performance. Sci. Total Environ. 732, 139206 https://doi.org/10.1016/j.scitotenv.2020.139206.

López-Vicente, M., Navas, A., 2009. Predicting soil erosion with RUSLE in Mediterranean agricultural systems at catchment scale. Soil Sci. 174 (5), 272–282. https://doi.org/10.1097/SS.0b013e3181a4bf50.

López-Vicente, M., Kramer, H., Keesstra, S., 2021. Effectiveness of soil erosion barriers to reduce sediment connectivity at small basin scale in a fire-affected forest. J. Environ. Manag. 278 (Part 1), 111510 https://doi.org/10.1016/j.jenvman.2020.111510.

Lucas-Borja, M.E., Van Stan II, J.T., Heydari, M., Omidipour, R., Rocha, F., Plaza-Alvarez, P.A., Zema, D.A., Muñoz-Rojas, M., 2021. Post-fire restoration with contour-felled log debris increases early recruitment of Spanish black pine (Pinus nigra Arn. ssp. salzmannii) in Mediterranean forests. Restor. Ecol. 29 https://doi.org/10.1111/rec.13338.

Machida, W.S., Gomes, L., Moser, P., Castro, I.B., Miranda, S.C., da Silva-Júnior, M.C., Bustamante, M.M., 2021. Long term post-fire recovery of woody plants in savannas of central Brazil. For. Ecol. Manag. 493, 119255 https://doi.org/10.1016/j.foreco.2021.119255.

Maia, P., Pausas, J.G., Vasques, A., Keizer, J.J., 2012. Fire severity as a key factor in post-fire regeneration of Pinus pinaster (Ait.) in Central Portugal. Ann. For. Sci. 69, 489–498. https://doi.org/10.1007/s13595-012-0203-6.

Martínez-Murillo, J.F., López-Vicente, M., 2018. Effect of salvage logging and check dams on simulated hydrological connectivity in a burned area. Land Degrad. Dev. 29 (3), 701–712. https://doi.org/10.1002/ldr.2735.

Molinas-González, C.R., Castro, J., Leverkus, A.B., 2017. Deadwood decay in a burnt Mediterranean pine reforestation. Forests 8 (5), 158. https://doi.org/10.3390/f8050158.

Nearing, M.A., 2013, Soil Erosion and Conservation (Book Chapter). In: Environmental Modelling: Finding Simplicity in Complexity: Second Edition (Book Editors: John Wainwright and Mark Mulligan). Published by John Wiley & Sons, Ltd., pp. 365–378. https://doi.org/10.1002/9781118351475.ch22.

Nemens, D.G., Varner, J.M., Kidd, K.R., Wing, B., 2018. Do repeated wildfires promote restoration of oak woodlands in mixed-conifer landscapes? For. Ecol. Manag. 427, 143–151. https://doi.org/10.1016/j.foreco.2018.05.023.

Nunes, J.P., Malvar, M., Benali, A.A., Rial Rivas, M.E., Keizer, J.J., 2016. A simple water balance model adapted for soil water repellency: application on Portuguese burned and unburned eucalypt stands. Hydrol. Process. 30, 463–478. https://doi.org/10.1002/hyp.10629.

Panagos, P., Borrelli, P., Meusburger, K., Alewell, C., Lugato, E., Montanarella, L., 2015. Land Use Policy Estimating the soil erosion cover-management factor at the European scale. Land Use Policy 48, 38–50. https://doi.org/10.1016/j.landusepol.2015.05.021.

Pausas, J.G., Bond, W.J., 2020. On the three major recycling pathways in terrestrial ecosystems. Trends Ecol. Evol. 35 (9), 767–775. https://doi.org/10.1016/j.tree.2020.04.004.

Pérez-de-los-Reyes, C., Bravo, S., Amoros, J.A., Garcia-Navarro, F.J., Garcia-Pradas, J., Sanchez-Ormeño, M., Jiménez-Ballesta, R., 2020. The stony phase as a differentiation factor in vineyard soils. Span. J. Soil Sci. 10 (3), 237–247. https://doi.org/10.3232/SJSS.2020.V10.N3.07.

Picchio, R., Neri, F., Petrini, E., Verani, S., Marchi, E., Certini, G., 2012. Machinery-induced soil compaction in thinning two pine stands in central Italy. For. Ecol. Manag. 285, 38–43. https://doi.org/10.1016/j.foreco.2012.08.008.

Pierson, F.B., Moffet, C.A., Williams, C.J., Hardegree, S.P., Clark, P.E., 2009. Prescribed-fire effects on rill and interrill runoff and erosion in a mountainous sagebrush landscape. Earth Surf. Process. Landf. 34 (2), 193–203. https://doi.org/10.1002/esp.1703.

Pivello, V.R., Vieira, I., Christianini, A.V., Ribeiro, D.B., da Silva Menezes, L., Berlinck, C. N., Melo, F.P.L., Marengo, J.A., Tornquist, C.G., Tomas, W.M., Overbeck, G.E., 2021. Understanding Brazil's catastrophic fires: causes, consequences and policy needed to prevent future tragedies. Perspect. Ecol. Conserv. 19 (3), 233–255. https://doi.org/10.1016/j.pecon.2021.06.005.

Raftoyannis, Y., Spanos, I., 2005. Evaluation of log and branch barriers as post-fire rehabilitation treatments in a Mediterranean pine forest in Greece. Int. J. Wildland Fire 14 (2), 183–188. https://doi.org/10.1071/WF04031.

Robichaud, P.R., Ashmun, L.E., Sims, B.D., 2010. Post-fire treatment effectiveness for hillslope stabilization. USDA For. Serv. - Gen. Tech. Rep. RMRS-GTR 240, 1–62. https://doi.org/10.2737/RMRS-GTR-240.

Robichaud, P.R., Lewis, S.A., Wagenbrenner, J.W., Brown, R.E., Pierson, F.B., 2020. Quantifying long-term post-fire sediment delivery and erosion mitigation effectiveness. Earth Surf. Process. Landf. 45 (3), 771–782. https://doi.org/10.1002/esp.4755.

Robichaud, P.R., Storrar, K.A., Wagenbrenner, J.W., 2019. Effectiveness of straw bale check dams at reducing post-fire sediment yields from steep ephemeral channels. Sci. Total Environ. 676, 721–731. https://doi.org/10.1016/j.scitotenv.2019.04.246.

Robichaud, P.R., Wagenbrenner, J.W., Brown, R.E., Wohlgemuth, P.M., Beyers, J.L., 2008. Evaluating the effectiveness of contour-felled log erosion barriers as a post-fire runoff and erosion mitigation treatment in the western United States. Int. J. Wildland Fire 17 (2), 255–273. https://doi.org/10.1071/WF07032.

Robinne, F.-N., Hallema, D.W., Bladon, K.D., Buttle, J.M., 2020. Wildfire impacts on hydrologic ecosystem services in North American high-latitude forests: a scoping review. J. Hydrol. 581, 124360 https://doi.org/10.1016/j.jhydrol.2019.124360.

Rodrigues, M., Ibarra, P., Echeverría, M., Pérez-Cabello, F., de la Riva, J., 2014. A method for regional-scale assessment of vegetation recovery time after high-severity wildfires: case study of Spain. Prog. Phys. Geogr.: Earth Environ. 38 (5), 556–575 https://doi.org/10.1177%2F0309133314542956.

Ruokolainen, L., Salo, K., 2009. The effect of fire intensity on vegetation succession on a sub-xeric heath during ten years after wildfire. Ann. Bot. Fenn. 46 (1), 30–42. https://doi.org/10.5735/085.046.0103.

Rutherford, M.C., Powrie, L.W., Husted, L.B., Turner, R.C., 2011. Early post-fire plant succession in Peninsula Sandstone Fynbos: the first three years after disturbance. South Afr. J. Bot. 77 (3), 665–674. https://doi.org/10.1016/j.sajb.2011.02.002.

Salesa, D., Cerdà, A., 2020. Soil erosion on mountain trails as a consequence of recreational activities. A comprehensive review of the scientific literature. J. Environ. Manag. 271, 110990 https://doi.org/10.1016/j.jenvman.2020.110990.

Salesa, D., Terol, E., Cerdà, A., 2019. Soil erosion on the "El Portalet" mountain trails in the Eastern Iberian Peninsula. Sci. Total Environ. 661, 504–513. https://doi.org/10.1016/j.scitotenv.2019.01.192.

Savadogo, P., Sawadogo, L., Tiveau, D., 2007. Effects of grazing intensity and prescribed fire on soil physical and hydrological properties and pasture yield in the savanna woodlands of Burkina Faso. Agric., Ecosyst. Environ. 118 (1–4), 80–92. https://doi.org/10.1016/j.agee.2006.05.002.

Sheridan, G.J., Lane, P.N.J., Sherwin, C.B., Noske, P.J., 2011. Post-fire changes in sediment rating curves in a wet Eucalyptus forest in SE Australia. J. Hydrol. 409 (1–2), 183–195. https://doi.org/10.1016/j.jhydrol.2011.08.016.

Shin, J.-I., Seo, W.-W., Kim, T., Park, J., Woo, C.-S., 2019. Using UAV multispectral images for classification of forest burn severity – a case study of the 2019 Gangneung forest fire. Forests 10 (11), 1025. https://doi.org/10.3390/f10111025.

Stephenson, C., Handmer, J., Betts, R., 2013. Estimating the economic, social and environmental impacts of wildfires in Australia. Environ. Hazards 12 (2), 93–111. https://doi.org/10.1080/17477891.2012.703490.

Talucci, A.C., Forbath, E., Kropp, H., Alexander, H.D., DeMarco, J., Paulson, A.K., Zimov, N.S., Zimov, S., Loranty, M.M., 2020. Evaluating post-fire vegetation recovery in Cajander Larch Forests in Northeastern Siberia using UAV derived vegetation indices. Remote Sens. 12 (18), 2970. https://doi.org/10.3390/rs12182970.

Vega, S.G.-D., de las Heras, J., Moya, D., 2018. Post-fire regeneration and diversity response to burn severity in Pinus halepensis Mill. Forests 9 (6), 299. https://doi.org/10.3390/f9060299.

Viana-Soto, A., Aguado, I., Salas, J., García, M., 2020. Identifying post-fire recovery trajectories and driving factors using landsat time series in fire-prone Mediterranean pine forests. Remote Sens. 12 (9), 1499 https://doi.org/10.3390/rs12091499.

Viedma, O., Chico, F., Fernández, J.J., Madrigal, C., Safford, H.D., Moreno, J.M., 2020. Disentangling the role of prefire vegetation vs. burning conditions on fire severity in a large forest fire in SE Spain. Remote Sens. Environ. 247, 111891 https://doi.org/10.1016/j.rse.2020.111891.

Volkova, L., Roxburgh, S.H., Weston, C.J., 2021. Effects of prescribed fire frequency on wildfire emissions and carbon sequestration in a fire adapted ecosystem using a comprehensive carbon model. J. Environ. Manag. 290, 112673 https://doi.org/10.1016/j.jenvman.2021.112673.

Wilson, C., Kampf, S.K., Ryan, S., Covino, T., MacDonald, L.H., Gleason, H., 2021. Connectivity of post-fire runoff and sediment from nested hillslopes and watersheds. Hydrol. Process. 35 (1), e13975 https://doi.org/10.1002/hyp.13975.

Wittenberg, L., van der Wal, H., Keesstra, S., Tessler, N., 2020. Post-fire management treatment effects on soil properties and burned area restoration in a wildland-urban interface, Haifa Fire case study. Sci. Total Environ. 716, 135190 https://doi.org/10.1016/j.scitotenv.2019.135190.

Wohlgemuth, P.M., Hubbert, K.R., Robichaud, P.R., 2001. The effects of log erosion barriers on post-fire hydrologic response and sediment yield in small forested watersheds, southern California. Hydrol. Process. 15 (15), 3053–3066. https://doi.org/10.1002/hyp.391.